

Multi-omics profiling of cross-resistance between ceftazidime-avibactam and meropenem identifies common and strain-specific mechanisms in *Pseudomonas aeruginosa* clinical isolates

Journal Article

Author(s):

Bartmanski, Bartosz J.; Bösch, Anja; Schmitt, Steven; Ireddy, Niranjan R.; Ren, Qun; Findlay, Jacqueline; Egli, Adrian; Zimmermann-Kogadeeva, Maria; Babouee Flury, Baharak

Publication date:

2025-07-09

Permanent link:

<https://doi.org/https://doi.org/10.3929/ethz-b-000739418>

Rights / license:

[Creative Commons Attribution 4.0 International](#)

Originally published in:

mBio 16(7), <https://doi.org/10.1128/mbio.03896-24>

Multi-omics profiling of cross-resistance between ceftazidime-avibactam and meropenem identifies common and strain-specific mechanisms in *Pseudomonas aeruginosa* clinical isolates

Bartosz J. Bartmanski,¹ Anja Bösch,^{2,3} Steven Schmitt,⁴ Niranjana R. Ireddy,^{2,3,5} Qun Ren,⁶ Jacqueline Findlay,⁷ Adrian Egli,⁸ Maria Zimmermann-Kogadeeva,¹ Baharak Babouee Flury^{2,3,9}

AUTHOR AFFILIATIONS See affiliation list on p. 21.

ABSTRACT *Pseudomonas aeruginosa* is a highly versatile and resilient pathogen that can infect different tissues and rapidly develop resistance to multiple drugs. Ceftazidime-avibactam (CZA) is an antibiotic often used to treat multidrug-resistant infections; however, the knowledge on the CZA resistance mechanisms in *P. aeruginosa* is limited. Here, we performed laboratory evolution of eight clinical isolates of *P. aeruginosa* exposed to either CZA or meropenem (MEM) in sub-inhibitory concentrations and used multi-omics profiling to investigate emerging resistance mechanisms. The majority of strains exposed to MEM developed high resistance (83%, 20/24 strains from eight clinical isolates), with only 17% (4/24) acquiring cross-resistance to CZA. The rate of resistance evolution to CZA was substantially lower (21%, 5/24), while 38% (9/24) acquired cross-resistance to MEM. Whole-genome sequencing revealed strain heterogeneity and different evolutionary paths, with three genes mutated in three or more strains: *dacB* in CZA-treated strains and *oprD* and *ftsI* in MEM-treated strains. Transcriptomic and proteomic analysis underlined heterogeneous strain response to antibiotic treatment with few commonly regulated genes and proteins. To identify genes potentially associated with antibiotic resistance, we built a machine learning model that could separate CZA- and MEM-resistant from sensitive strains based on gene expression and protein abundances. To test some of the identified associations, we performed CRISPR-Cas9 genome editing that demonstrated that mutations in *dacB*, *ampD*, and, to a lesser extent, in *mexR* directly affected CZA resistance. Overall, this study provides novel insights into the strain-specific molecular mechanisms regulating CZA resistance in *Pseudomonas aeruginosa*.

IMPORTANCE *Pseudomonas aeruginosa* is one of the most difficult-to-treat pathogens in the hospital, which often acquires resistance to multiple antibiotics. Ceftazidime-avibactam (CZA) is an essential antibiotic used to treat multidrug-resistant infections, but its resistance mechanisms are not well understood. Here we investigated the evolution of resistance to CZA and meropenem (MEM) in eight clinical bacterial isolates from patients' blood, urine, and sputum. While the rate of resistance evolution to MEM was higher than to CZA, MEM-resistant strains rarely acquired cross-resistance toward CZA. To identify changes at the genome, transcriptome, and proteome levels during antibiotic exposure, we performed multi-omics profiling of the evolved strains and confirmed the effect of several genes on antibiotic resistance with genetic engineering. Altogether, our study provides insights into the molecular response of *P. aeruginosa* to CZA and MEM and informs therapeutic interventions, suggesting that CZA could still be effective for patients infected with MEM-resistant pathogens.

Editor Laurence Rahme, Massachusetts General Hospital, Boston, Massachusetts, USA

Address correspondence to Maria Zimmermann-Kogadeeva, maria.zimmermann@embl.de, or Baharak Babouee Flury, Baharak.BaboueeFlury@hoch.ch.

Bartosz J. Bartmanski and Anja Bösch contributed equally to this article. The order of these two authors was chosen based on their contribution in analyses and writing of the article.

The authors declare no conflict of interest.

See the funding table on p. 21.

This work has been presented at the 34th Congress of the European Society of Clinical Microbiology and Infectious Diseases in Barcelona, Spain (EO243) and the Joint Annual Meeting of the Swiss Society of Infectious Diseases and Microbiology in Bern, Switzerland (O077).

Received 15 January 2025

Accepted 1 May 2025

Published 4 June 2025

Copyright © 2025 Bartmanski et al. This is an open-access article distributed under the terms of the [Creative Commons Attribution 4.0 International license](https://creativecommons.org/licenses/by/4.0/).

KEYWORDS *Pseudomonas aeruginosa*, ceftazidime-avibactam, meropenem, resistance mechanisms, genomics, transcriptomics, proteomics, machine learning, CRISPR/Cas9, *dacB*

Pseudomonas aeruginosa is an opportunistic pathogen causing serious infections in hospitalized patients, including chronic respiratory infections in patients with cystic fibrosis (1). This pathogen can adapt to diverse ecological niches (2, 3) and is considered a difficult-to-treat pathogen because of its versatile antibiotic resistance mechanisms, hypermutable strains, and antibiotic-tolerant cells (4–7).

Given the high prevalence of multidrug resistance (MDR) in *P. aeruginosa*, appropriate antibiotic selection is essential. Acute, life-threatening infections must be treated immediately, while antibiotic susceptibility testing results of clinical isolates often take up to 3 days to obtain (8). Empiric treatment often includes beta-lactam antibiotics, such as piperacillin-tazobactam, broad-spectrum cephalosporins, or carbapenems such as meropenem (MEM) (9). Despite their notable efficacy against *P. aeruginosa* (8, 10), multiple resistance mechanisms against these antibiotics have emerged (11–14). Ceftazidime-avibactam (CZA), which combines ceftazidime with a non-beta-lactam beta-lactamase inhibitor, became a promising treatment option with broad-spectrum activity against MDR pathogens (15, 16). The introduction of CZA has not been without setbacks. Soon after its release, resistance was described in *Klebsiella pneumoniae* isolates (17, 18). Resistance to CZA has also been described *in vitro* in *P. aeruginosa* that were incubated in the presence of increasing concentrations of CZA. All resistant variants exhibited mutations in their *ampC*, mainly in the Omega-loop region (19). In addition, cross-resistance to CZA was revealed in *P. aeruginosa* with single nucleotide polymorphisms (SNPs) in *ampC* and *ampR*, which led to ceftolozane-tazobactam resistance (20, 21).

Multi-omics, including transcriptomics or proteomics, is increasingly used to study antibiotic resistance mechanisms across molecular layers (22–24). Complex antibiotic responses reported in *P. aeruginosa* and other pathogens range from changes in energy metabolism, ribosomal activity, and DNA metabolism to peptidoglycan biosynthesis and stress response (25, 26). While CZA responses include derepression of cephalosporinase AmpC, efflux pump upregulation, porin loss/modification, and deficiencies in DNA mismatch repair (27), the exact resistance mechanisms remain unclear (28–30). Another important aspect of managing *P. aeruginosa* infections is the understanding of cross-resistance evolution, particularly in cases previously treated with MEM. This information is essential for rapid clinical decision-making, but relevant data on this topic are currently lacking.

This study aims to elucidate resistance and cross-resistance mechanisms to MEM and CZA in *P. aeruginosa* through *in vitro* evolution experiments, multi-omics profiling, and genome engineering, offering valuable insights for physicians selecting empirical treatments for *P. aeruginosa* infections pre-treated with meropenem. Additionally, it highlights *P. aeruginosa* strategies for MEM and CZA adaptation and resistance, which could guide the development of new antibiotics and combination therapies.

RESULTS

Experimental evolution of antimicrobial resistance to MEM and CZA in clinical isolates

To investigate the evolution of resistance and cross-resistance to MEM and CZA in *P. aeruginosa*, we collected eight clinical isolates from three different infection locations (blood, sputum, and urine), confirmed their sensitivity to the drugs (Table S1), and exposed them to sub-inhibitory concentrations of either drug for 18 days in triplicate (Fig. 1A). We observed that among the strains exposed to sub-inhibitory levels of CZA, 21% (5/24) became resistant to CZA, while 38% (9/24) demonstrated the development of cross-resistance to MEM in accordance with the European Committee on Antimicrobial Susceptibility Testing (EUCAST) resistance breakpoint guidelines of minimal inhibitory

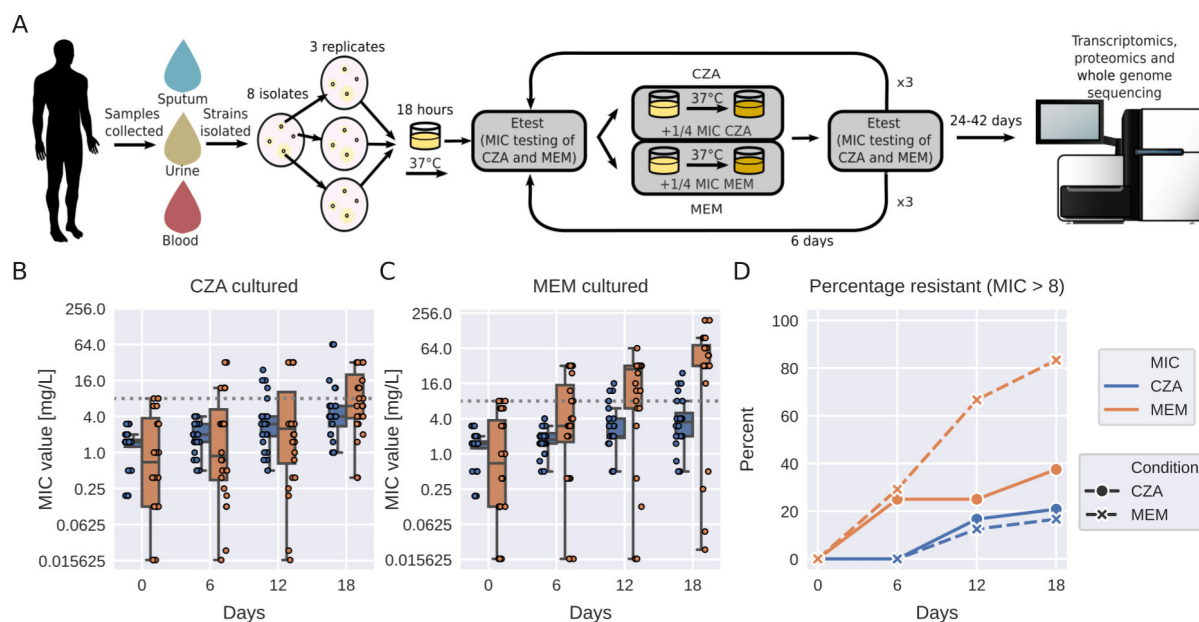


FIG 1 Experimental evolution of antimicrobial resistance to MEM and CZA in clinical isolates. (A) Experimental design. (B) Resistance evolution to MEM and CZA in strains exposed to CZA. (C) Resistance evolution to MEM and CZA in strains exposed to MEM. (D) Percentage of MEM- and CZA-resistant strains (MIC > 8 mg/L) among strains exposed to either MEM or CZA. In panels B and C, the gray horizontal dotted line corresponds to the MIC = 8 mg/L threshold. Boxplots represent median and interquartile range (between the first and the third quartile), while the whiskers extend from the box to the farthest data point lying within 1.5× the interquartile range from the box for $n = 24$ points ($n = 8$ strains in triplicate). In panel A, genomessequencer-2 icon by DBCLS (<https://togotv.dbcls.jp/en/pics.html>) is licensed under CC-BY 4.0 unported (<https://creativecommons.org/licenses/by/4.0/>). Petri-dish-with-colony-lightyellow icon by Servier (<https://smart.servier.com/>) is licensed under CC-BY 3.0 unported (<https://creativecommons.org/licenses/by/3.0/>).

concentration (MIC) >8 mg/L (31) (Fig. 1B; Fig. S1a). In contrast, most strains (20/24, 83%) subjected to sub-inhibitory concentrations of MEM acquired MEM resistance, with only a minority of 17% (4/24) concurrently displaying cross-resistance to CZA (Fig. 1C; Table S2). This observation also holds true if we consider a subset of five isolates which had a low initial MEM MIC (MIC ≤ 1 mg/L) (Fig. S1b). The increase of MIC was much higher for MEM compared to CZA (median increase of 32-fold and 5.3-fold versus 2.7-fold and 3-fold upon exposure to MEM and CZA, correspondingly; Table S2).

MEM and CZA induce distinct molecular responses across multi-omics layers

Given that only a minority, constituting 21% of the strains exposed to CZA, had exceeded the clinically defined resistance breakpoint of MIC >8 mg/L (31) after 18 days, we extended the evolutionary experiment for a longer period of time to capture the molecular mechanisms underlying the development of resistance. Specifically, one representative strain evolved from each of the parental isolates was subjected to sub-inhibitory concentrations of the respective antibiotics for a maximum of 42 days of continuous passaging. For technical reasons, we were able to collect the data from six strains evolved in CZA and five strains evolved in MEM out of eight parental strains. After this prolonged period, four out of six strains acquired CZA resistance (MIC > 8 mg/L), with two of them being cross-resistant to MEM (MIC > 8 mg/L) and one having the intermediate resistance. One of the CZA-sensitive strains also had intermediate MEM resistance. While all five MEM-exposed strains acquired high resistance (MIC > 96 mg/L), only two of them acquired CZA cross-resistance (Fig. 2A; Table S3). Notably, during exposure to MEM and CZA, strains also evolved resistance to other beta-lactams, cephalosporins, and other antibiotics (Table S4).

For all the parent and the evolved strains, we performed whole-genome sequencing and transcriptomics and proteomics analysis with three technical replicates to

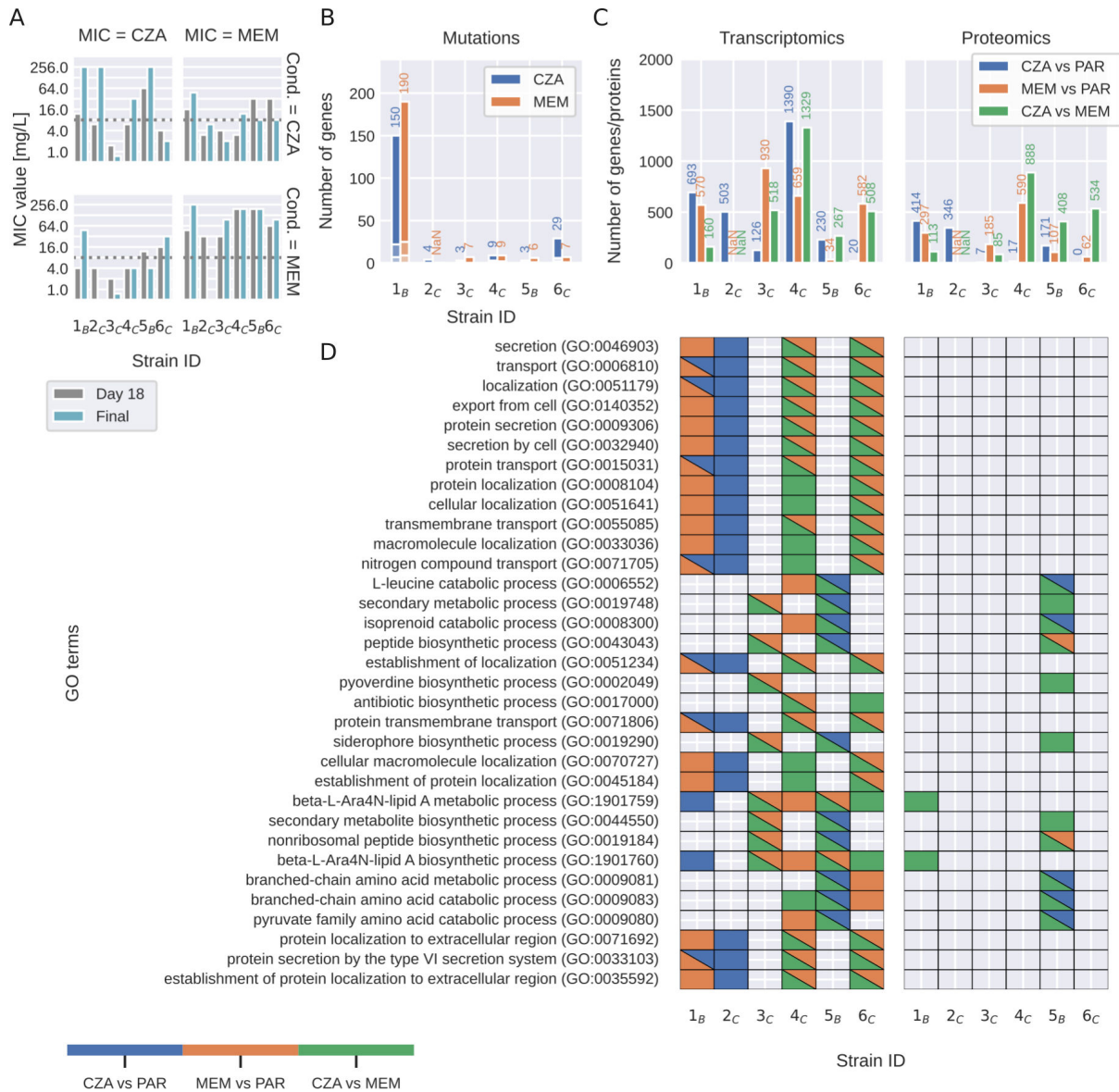


FIG 2 Molecular responses to MEM and CZA exposure across clinical isolates. (A) MIC values for strains exposed to either CZA or MEM after the initial 18 days of passaging and after 24–42 days of passaging. (B) Number of mutations induced by MEM or CZA exposure (depicts the sum of all types of detected mutations, such as SNP, insertion, deletion, and complex rearrangements). (C) Number of differentially expressed genes and differentially abundant proteins induced by MEM or CZA exposure compared to parent strains (PAR) [$\log_2(\text{fold change}) \geq 1$, false discovery rate (FDR) ≤ 0.05 determined using Wald test and unpaired two-sided moderated *t*-test for gene expression and protein abundance, respectively, and adjusted with Benjamini-Hochberg procedure]. (D) GO enrichment analysis of differentially abundant genes and proteins. Color highlights significantly enriched GO terms (FDR ≤ 0.05). For visualization purposes, only GO terms that pass a significance threshold of FDR ≤ 0.001 in at least two strains for transcriptomics or in at least one strain for proteomics are shown.

investigate acquired mutations and changes in gene expression and protein abundance upon antibiotic treatment.

Whole-genome sequencing revealed that the six strains carried five sequence types and were genetically diverse, representing different clades of the *P. aeruginosa* phylogenetic tree (Fig. S2 and S3). Most evolved strains accumulated a similar number of mutations when exposed to MEM or CZA (between 3 and 29), while one of the strains (1_B) was a hypermutable strain, accumulating more than 150 mutations (Fig. 2B; Table S5). Several genes acquired mutations independently in several strains or in the same strain exposed to either of the drugs. The most frequently mutated genes were penicillin-binding proteins *ftsI* (in two strains exposed to CZA and four strains exposed to MEM)

and *dacB* (in four strains exposed to CZA). These were followed by outer membrane protein *oprD* (in three strains exposed to MEM), two-component system sensor *phoQ* (in two strains exposed to MEM and one strain exposed to CZA), and multidrug efflux pump *mexB* and its regulator *mexR* (in one strain exposed to CZA and two strains exposed to MEM) (Table S5). However, none of the mutations could be unambiguously attributed to the levels of acquired CZA or MEM resistance.

Exposure to MEM or CZA induced large changes in gene expression {up to 1,390 differentially expressed genes across strains, $\text{abs}[\log_2(\text{fold change})] > 1$, false discovery rate (FDR)-adjusted P -value < 0.05 } and protein abundance {up to 888 differentially abundant proteins, $\text{abs}[\log_2(\text{fold change})] > 1$, FDR-adjusted P -value < 0.05 } (Fig. 2C; Tables S6 and S7; Fig. S3 and S4). While gene and protein responses were distinct between the two drugs (up to 1,329 differentially expressed genes and 888 differentially abundant proteins per strain between MEM and CZA conditions), gene ontology enrichment analysis revealed several common processes affected by either of the antibiotic treatments. These included membrane transport, protein secretion, and cellular localization. Furthermore, exposure to CZA and MEM affected amino acid, lipid, and nonribosomal peptide metabolic processes in different strains (Fig. 2D; Table S8).

While we observed some common responses to MEM and CZA exposure between strains, there was no process that could be unambiguously attributed to antimicrobial resistance. For example, while several genes involved in protein transport, localization, and secretion were regulated in CZA-resistant strains 1_B and 2_C upon CZA exposure, they were not enriched among genes regulated by the two other resistant strains, 4_C and 5_B. The response to CZA of the highly CZA-resistant strain 5_B was unique to this strain and characterized mainly by the changes in biosynthetic and metabolic processes. Therefore, we next set out to compare molecular changes across strains in more detail to identify potential antibiotic resistance features.

Molecular signatures of evolved strains are largely specific to the parental strain

To compare molecular signatures between strains and conditions, we performed dimensionality reduction of the normalized transcriptomics and proteomics profiles with principal component analysis (PCA). This analysis revealed that the evolved strains exposed to either MEM or CZA grouped together with the parental strain, underlining that the parental strain determined the global transcriptional and protein abundance profiles of the evolved strains more than the antibiotic exposure (Fig. 3A). We note that due to insufficient sample quality, we had to exclude the MEM-evolved 2_C strain from our analysis.

Indeed, while MEM or CZA treatment induced large transcriptional (1,895 or 2,178 out of 5,563 detected genes) and protein (984 or 809 out of 4,028 detected proteins) changes across strains, most of these changes were strain-specific (Fig. 3B; Tables S6, S7, and S9). MEM induced more common transcriptional and protein changes across strains than CZA. About 41% of proteins changing upon MEM exposure (401 out of 984) and 40% of proteins changing upon CZA exposure (320 out of 809) were also changing on the transcript levels. They were mainly enriched in the nucleic acid metabolic processes, phenazine biosynthesis, and nitrogen compound transport (GO:0090304, GO:0002047, and GO:0071705) in MEM, and pyruvate family amino acid and branched-chain amino acid catabolic processes in CZA (GO:0009080 and GO:0009083; Table S8). The only genes significantly upregulated by four strains upon MEM treatment were *mexA* and *mexB*, and the corresponding proteins were upregulated as well (Fig. 3B; Table S9). While no proteins were differentially abundant in more than three strains cultured in CZA, there were seven genes that were significantly upregulated or downregulated in five strains cultured in CZA: porin B *oprB* (PA3186), beta-lactamase *ampC* (PA4110), and ribosomal protein S3AE (PA4111), as well as four genes belonging to an operon of ABC transporter genes PA3187–PA3190 (Table S9). Since these genes were differentially expressed in both CZA-resistant and sensitive strains, they are likely not unambiguously determining

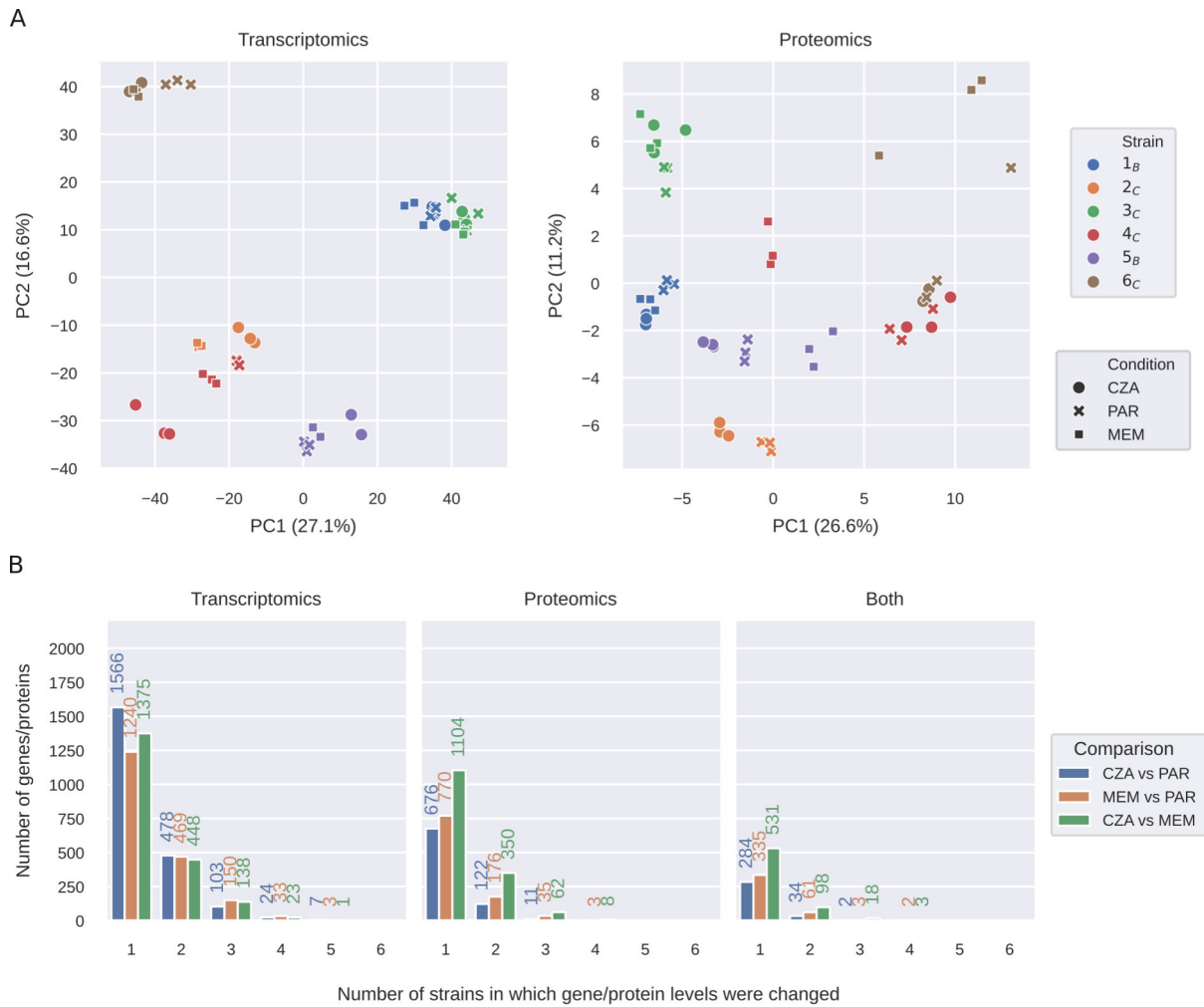


FIG 3 Molecular signatures of evolved strains are largely specific to the parental strain. (A) PCA plots of normalized transcriptomics and proteomics data for the parent strains and strains evolved in MEM or CZA. (B) Number of differentially expressed transcripts, differentially abundant proteins, or both shared between each number of strains [$\log_2(\text{fold change}) \geq 1$, $\text{FDR} \leq 0.05$ determined using Wald test and unpaired two-sided t -test for gene expression and protein abundance, respectively, and adjusted with Benjamini–Hochberg procedure]. PAR refers to parental strains.

resistance, but reflecting the stress response and bacterial attempts to extrude the antibiotic. To put the findings observed for the six clinical isolates into a broader perspective, we leveraged publicly available data sets on *P. aeruginosa* PAO1 strain exposed to MEM (32, 33), as well as transcriptomic profiles of large clinical isolate collections tested for MEM or CZA resistance (34, 35). While *mexA* was highly expressed in CZA-resistant strains and not differentially expressed by MEM-treated PAO1 strain, *ampC* and PA4111 were highly expressed both in MEM-resistant strains and in PAO1 treated with MEM. Three more genes out of the nine genes discussed above were also upregulated in the PAO1 strain in response to MEM (PA3186–PA3188; Table S10), supporting that they are rather markers of MEM response but not unambiguous resistance determinants. *P. aeruginosa* PAO1 response to MEM shared up to 40% of differentially expressed genes with the clinical isolates, providing an additional reference for general drug response of an antibiotic-sensitive strain (Fig. S6; Table S11).

A machine learning model identifies genes and proteins predictive of MEM and CZA resistance

To investigate whether MEM- or CZA-resistant strains have distinctive molecular signatures, we used a machine learning method, partial least squares-discriminant

analysis (PLS-DA), which is widely applied for discriminative analysis and classification in high-dimensional data sets (36, 37). PLS-DA aims to maximize the covariance between the sample class (defined as high resistance to CZA or MEM, MIC \geq 32 mg/L) and the predictor features (gene expression or protein abundance) and extracts latent features (latent factors) that capture the essential information for discriminating between the two classes. First, we built four PLS-DA models (for each of the two antibiotics and each of the two omics data types) using the full data set, including parent and CZA- and MEM-evolved strains (51 samples per model). All four models could separate resistant from sensitive strains with high accuracy (accuracy 0.96 and higher) (Fig. 4A; Table S12). To test the generalizability of the models, we performed a leave-one-strain-out analysis, where each of the models was trained on the data from five strains (42–45 samples) and tested on the data from the sixth strain not included in the training (six to nine samples) (Fig. 4B). Reflecting the heterogeneity between strains, resistance prediction accuracy substantially varied depending on which strain was left out (Fig. 4C). Both MEM- and CZA-resistance models trained on proteomics data achieved higher accuracy than models trained on transcriptomics data (median accuracies 0.72 and 0.67 compared to 0.67 and 0.36; Table S12).

We then took advantage of the latent factor projections calculated by PLS-DA to identify genes and proteins most informative for the prediction of each model. For each of the gene or protein features, we calculated how many leave-one-strain-out models included this feature among the top 100 features sorted by the latent factor projection coefficients (out of 5,563 total features for transcriptomics and 1,923 total features for proteomics). While most of the top predictive features were model-specific, we identified small subsets of features that were repeatedly picked by five or all six leave-one-strain-out models of each type (Fig. 4D; Table S12). For MEM resistance prediction, the models based on transcriptomics picked genes involved in membrane functions, while most frequently picked proteins were involved in metabolic processes, specifically carbohydrate derivative, carnitine, and dTDP-rhamnose metabolism (Fig. 4E; Table S12). For CZA resistance prediction, the selected gene features were attributed to aminoglycan and peptidoglycan catabolic processes, while protein features were involved in gene expression, protein folding, and cysteinyl-tRNA aminoacylation (Fig. 4E; Table S12). We then focused on the features selected by five or more MEM- or CZA-predicting models (40 and 24 features correspondingly; Fig. 4D), and filtered them further by calculating whether they were significantly differentially expressed between CZA-sensitive and resistant strains (FDR \leq 0.01; Table S13). This resulted in nine features for MEM resistance and 12 features for CZA resistance (Fig. S5 and S6; Table S14). Among the 12 CZA-resistance features, three genes were reported to affect resistance to different antibiotics in a genome-wide transposon mutant study (30) (Table S14). Two of these genes are associated with alginate biosynthesis (PA0460 and PA0764 [*mucB*]), while the third one, glutathione hydrolase proenzyme *ggt* (PA1338), was also reported to be downregulated in a gentamicin-resistant clinical isolate (38). Alginate and other exopolysaccharides are known to affect biofilm formation, pathogenicity, and antibiotic resistance (39–42). The other genes from the list are involved in cell wall biosynthesis (PA4421 [*mraZ*]) or metabolic functions (PA2197, PA3945, PA4847 [*accB*], PA3082 [*gbt*], PA5556 [*atpA*]) and have been associated with virulence, antibiotic response, or resistance (43–47), while the upregulated selenide, water dikinase *selD* (PA1642), was proposed as a drug target in *Klebsiella* (48) (Table S14). Overall, PLS-DA enabled the identification of transcriptomics and proteomics features that are associated with a higher resistance to MEM or CZA, which may include antibiotic resistance mechanisms, as well as stress response to the higher antibiotic levels in the antibiotic-resistant group, or general characteristics of highly pathogenic strains, such as biofilm formation capacities.

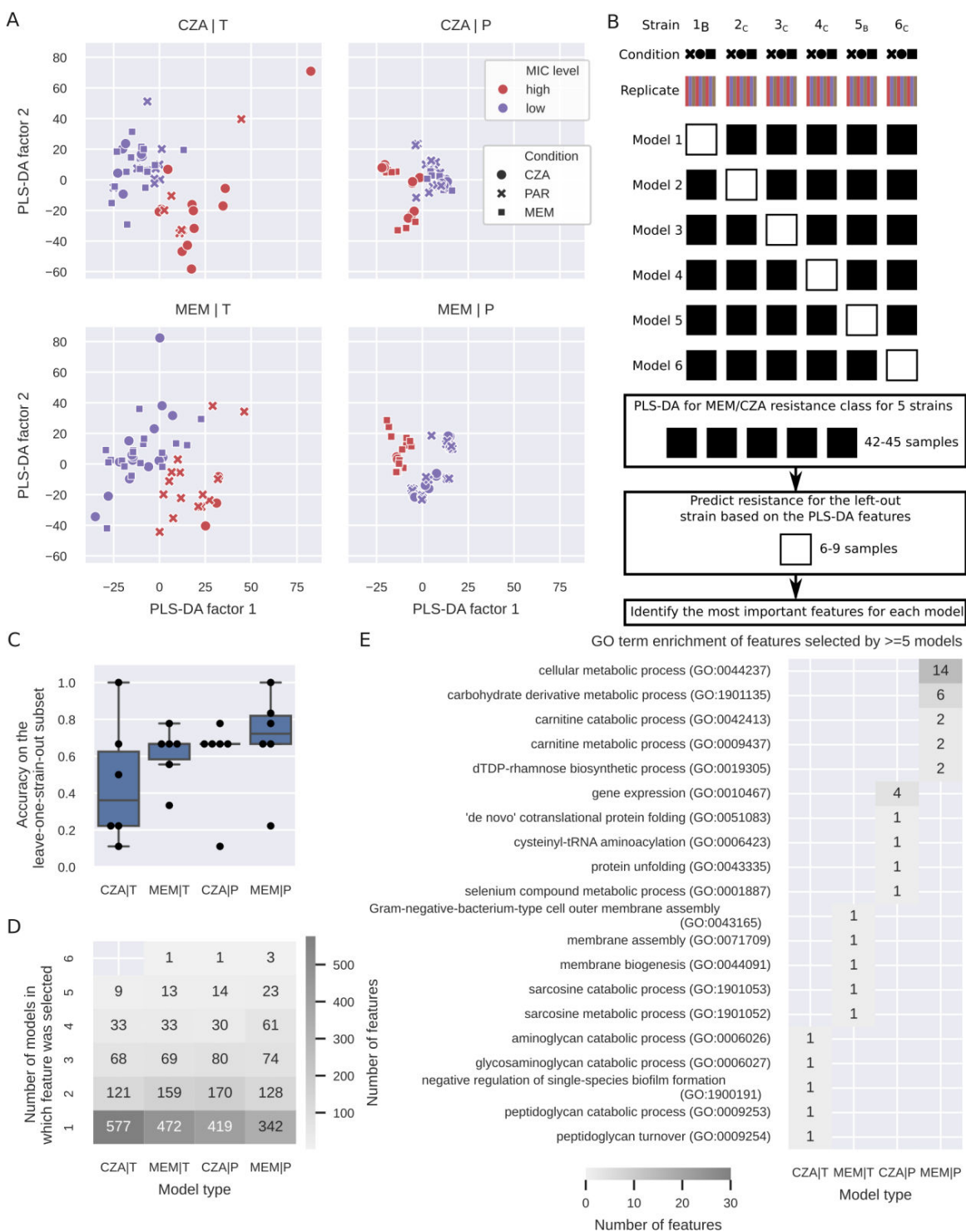


FIG 4 A machine learning model identifies genes and proteins predictive of MEM and CZA resistance. (A) PLS-DA plots for models built for transcriptomics (left) or proteomics (right) data to predict high CZA (top) or MEM (bottom) resistance (threshold at MIC \geq 32 mg/L). (B) Scheme of the leave-one-strain-out approach to identify genes and proteins predictive of CZA or MEM resistance. (C) Accuracy of the six leave-one-strain-out models on the leave-one-strain-out subset (calculated based on $n = 6-9$ samples for each left out strain) for each of the omics data types and antibiotics. (D) Number of predictive features selected by one to six of the leave-one-strain-out models (only top 100 features per model were considered for comparison). (E) GO enrichment analysis of features selected by ≥ 5 leave-one-strain-out models. The top 5 GO terms per model are shown sorted by the P -value. Only GO:1901135 passes the $FDR \leq 0.1$ threshold.

Antibiotic exposure-associated features span from membrane and transport processes to energy and lipopolysaccharide metabolism

To summarize antibiotic exposure-associated processes, we combined genes and proteins identified with mutation analysis, differential transcriptomic and proteomic analyses, as well as the PLS-DA models. From mutation analysis, we selected genes in which mutation occurred at least two times independently in our assay (19 genes); from differential analysis, we selected genes and proteins significantly upregulated or downregulated $\{|\text{abs}[\log_2(\text{fold change})]\} \geq 1$ in either of the omics, $\text{FDR} < 0.05$ in both omics by at least five strains from transcriptomics, four strains from proteomics, and three strains from both (17 genes/proteins). Lastly, from PLS-DA, we selected features that were highly important in at least five leave-one-strain-out models and additionally differentially abundant between sensitive and resistant strains ($\text{FDR} < 0.01$, 21 genes/proteins; Table S14). Since some genes or proteins were selected by multiple of these analyses, there were 56 features selected in total (Table S15).

Mutations most frequently occurred in penicillin-binding proteins *dacB* (only upon CZA treatment) and *ftsI* (both upon MEM and CZA treatment), while the expression of these genes was unchanged or decreased (Fig. 5; Table S15). The most pronounced upregulation both on the transcript and the protein levels was observed in the *mexAB-oprM* efflux system in the majority of strains exposed to MEM and two of the three strains which acquired high resistance to CZA. However, this upregulation was not coinciding with cross-resistance. Mutations were also detected in the *mexB* gene upon both CZA and MEM exposure, in the *nalD* gene that was reported to contribute to the increase of *mexAB-oprM* expression in *P. aeruginosa* (49), and in the *mexR* gene, recognized as a repressor gene of the *mexAB-oprM* multidrug efflux operon (50) (Fig. 5; Table S15). The expected antibiotic resistance determinant beta-lactamase *ampC* was upregulated in the majority of the strains exposed to CZA; however, it did not exclusively determine CZA resistance or cross-resistance, since both CZA-sensitive and resistant strains had high *ampC* expression levels according to the transcriptomic profiling.

Antibiotic exposure-associated genes and proteins belonging to the metabolism and energy production category were selected either by differential analysis or PLS-DA and were mainly downregulated, indicating that antibiotic exposure impaired the growth and metabolism of resistant strains more than sensitive strains, likely due to the differences in the administered antibiotic doses.

The two categories of genes/proteins identified by all three types of analysis were membrane proteins and outer membrane channels and polysaccharide and lipopolysaccharide metabolism (Fig. 5; Table S15). Mutations occurring within *oprD* were uniquely observed in strains exposed to MEM, but not coinciding with cross-resistance to CZA. The expression of *oprD* as well as the outer membrane protein *oprE* was generally downregulated (Fig. 5; Table S15). Genes involved in lipopolysaccharide metabolism were mutated mainly upon MEM exposure (the *phoP-phoQ* two-component regulatory system, murein peptide ligase *mpl*, and cell division protein *ftsZ*), while the expression of these and other genes in this category was generally increasing both upon MEM and CZA exposure.

To summarize, three types of analysis point toward mutations and expression changes in penicillin-binding proteins, efflux pump membrane proteins, as well as lipopolysaccharide metabolism genes as the most generally associated with antibiotic exposure, while highlighting drug-specific responses, such as mutations in *dacB* upon CZA exposure or *oprD* upon MEM exposure. These affected processes likely reflect not only antimicrobial resistance strategies but also bacterial stress response and general virulence factors.

CRISPR-Cas9 genome editing reveals that *dacB* mutation has a strong effect on CZA resistance

To test whether specific identified mutations can affect CZA or MEM resistance in *P. aeruginosa*, we set out to perform CRISPR-Cas9 genome editing of the *P. aeruginosa*

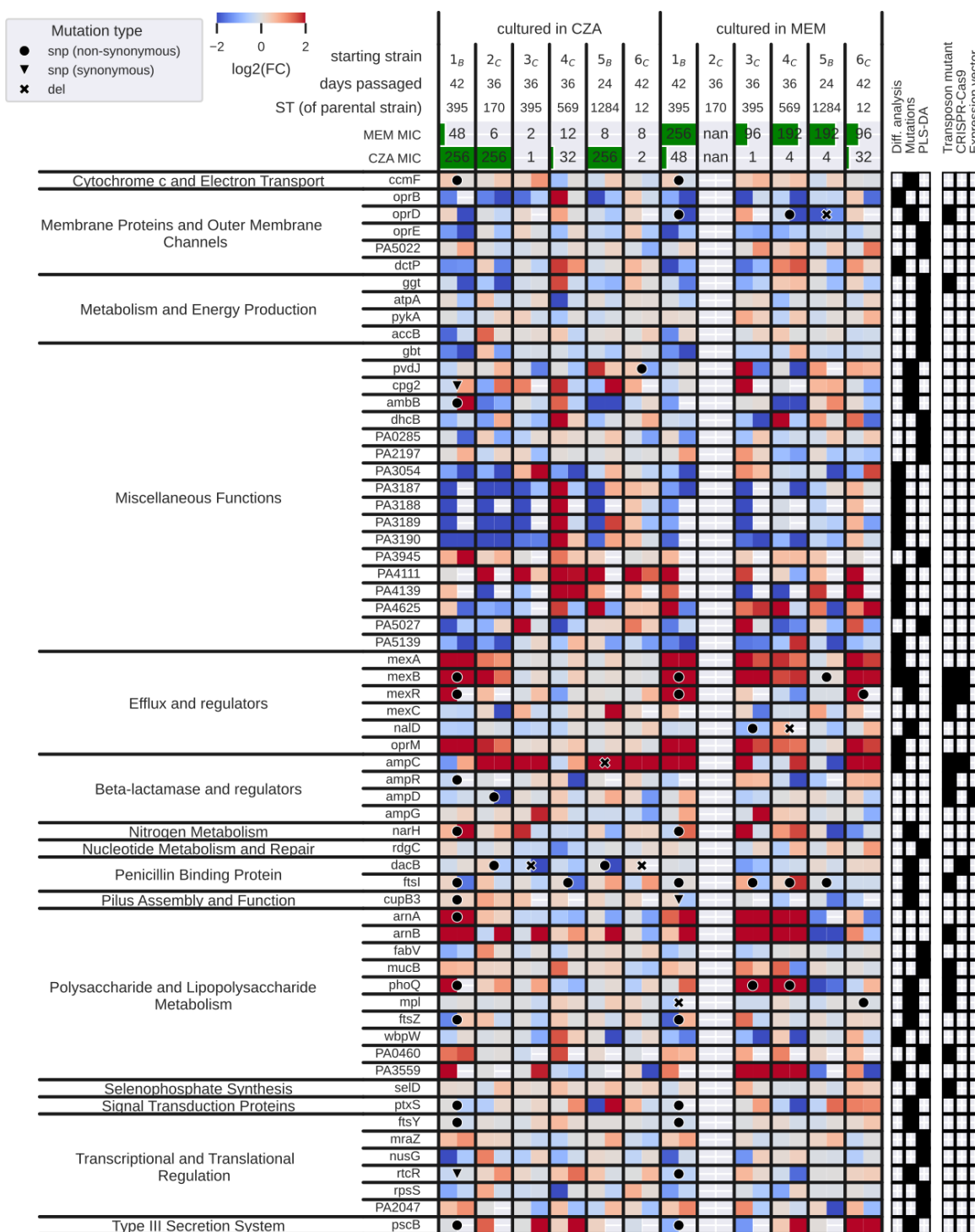


FIG 5 Overview of the antibiotic exposure-associated features identified by different types of analyses. The heatmap depicts transcriptomics log fold changes on the left and proteomics log fold changes on the right within each box for a given strain and gene. Red; upregulated, blue; downregulated. Mutations found for each gene in a given strain are depicted by a circle (non-synonymous SNP), a triangle (synonymous SNP), or a cross (deletion). The top 2 rows show the MIC values for CZA and MEM after the specified number of days. The panels on the right indicate the type of analysis through which each gene was identified (mutations, differential analysis, PLS-DA), and whether the gene was followed up in a CRISPR-Cas9, a transposon mutagenesis assay, or an expression vector cloning assay. Note that due to technical reasons, we removed the MEM-exposed 2_C strain from all the analyses.

mPAO1 strain using gene sequence templates from the highly resistant strains. Specifically, we focused on several of the most frequently mutated genes *dacB*, *mexB*, and *mexR*, the heavily upregulated *ampC*, and its regulator *ampD* (Fig. 5).

The mutations in *mexR* and *mexB* were introduced from strain 1_B, which exhibited high levels of resistance to both CZA and MEM. The introduction of the L13P (T38C) mutation in *mexR*, which is accompanied by a 20-fold increase in its expression upon MEM treatment of 1_B (Table S6), resulted in a threefold rise in MEM MIC and a twofold rise in CZA MIC, respectively. Introducing the R620C (C1858T) mutation in *mexB* led to a 1.5-fold increase in CZA MIC without affecting MEM MIC (Table 1).

For the *ampC* deletion introduced based on the template from isolate 5_B, we also observed a moderate increase of 1.5-fold in CZA resistance and no effect on MEM resistance (Table 1), likely explained by the fact that this deletion was upstream of the avibactam-binding site.

The strongest effect on CZA MIC was observed by introducing the *dacB* mutation acquired by strain 2_C exposed to CZA (Table 1): the CZA MIC increased fourfold, while no discernible impact on MEM resistance was detected. In contrast, introducing another *dacB* mutation from the CZA-resistant strain 5_B did not result in any changes in the MIC of either CZA or MEM (Table 1).

Overall, our CRISPR-Cas9 assays could confirm the effects on CZA resistance of *dacB* and *mexR*, although the effects were much less pronounced than the resistance patterns of the evolved strains. Along with CRISPR-Cas9 assays, we also performed MIC assays with a subset of transposon insertion mutants in the *P. aeruginosa* mPAO1 mutant library ($n = 15$ mutants; Fig. 5; Table S16). From the tested transposon mutants, we observed substantial differences to the wild-type CZA MIC in 2 out of 15: 25% reduction in MIC in *mexB* mutant and threefold increase in MIC in *mexR* mutant (Fig. S9; Table S16). These results underline the composite nature of antibiotic resistance mechanisms, as genetic perturbations of single genes cannot fully recapitulate the resistance phenotypes of the evolved strains.

Introduction of the wild-type *ampD* gene reversed CZA resistance in the mutant strain

As CRISPR-Cas9 genome editing was unsuccessful for the *ampD* mutation despite several attempts, we opted for an alternative approach. We cloned the wild-type *ampD* allele from the sensitive 2_C parent strain (CZA MIC = 2 mg/L) into the pUCP24 vector and introduced it into the evolved 2_C strain (CZA MIC = 128 mg/L) via transformation assays using *Escherichia coli* TOP10. Complementation with the parent *ampD* gene led to a 64-fold decrease of resistance in the mutant strain (CZA MIC = 2 mg/L; Table 2), confirming that *ampD* mutation was the leading cause of acquired CZA resistance in this strain.

DISCUSSION

Treatment of *P. aeruginosa* infections is challenging due to the versatility of strains and their potential to develop antimicrobial resistance. In this multi-omics, multi-assay investigation of the *in vitro* evolution of resistance to MEM and CZA in eight clinical *P.*

TABLE 1 Results of CZA and MEM resistance assays of the CRISPR-Cas9 edited mutants of *P. aeruginosa* mPAO1

Gene	Strain	Mutation	CZA MIC mPAO1	CZA MIC CRISPANT	CZA MIC fold change mPAO1	MEM MIC mPAO1	MEM MIC crispant	MEM MIC fold change
<i>dacB</i>	2 _C	c.1282A > C p.Thr428Pro	0.50	2.00	4.00	0.50	0.50	1.00
<i>dacB</i>	5 _B	c.1349T > A p.Val450Glu	0.50	0.50	1.00	0.50	0.50	1.00
<i>mexR</i>	1 _B	c.38T > C p.Leu13Pro	0.50	1.00	2.00	0.50	1.50	3.00
<i>mexB</i>	1 _B	c.1858C > T p.Arg620Cys	0.50	0.75	1.50	0.50	0.50	1.00
<i>ampC</i>	5 _B	c.711_731delACGGGTCCGGTCCCGGCCGCT p.Arg238_Leu244del	0.50	0.75	1.50	0.50	0.50	1.00

TABLE 2 CZA MIC of clinical isolates expressing *ampD* gene on a pUCP24 vector^a

Strain	Parent (2 _C)	Mutant (2 _C)	Parent/pUCP24	Mutant/pUCP24	Parent/pUCPampD	Mutant/pUCPampD
CZA MIC, mg/L	2	128	2	128	2	2

^aParent 2_C is the unevolved clinical isolate, mutant 2_C is the 2_C isolate evolved in MEM.

aeruginosa isolates, we addressed these challenges both from the clinical and from the systems microbiology perspectives.

From the clinical perspective, our observations revealed that strains subjected to sub-inhibitory concentrations of MEM exhibited a considerably higher rate of and faster resistance evolution compared to those exposed to CZA. This suggests prolonged/inappropriate MEM use may accelerate resistance, potentially diminishing its therapeutic efficacy. In contrast, CZA demonstrated a lower propensity for resistance development. These findings are in line with a recent study where *P. aeruginosa* isolates displayed greater increases in the mean MIC for MEM compared to CZA when subjected to increasing concentrations of the respective antibiotics (51).

Although cross-resistance to CZA appeared in fewer cases, continuous surveillance is important to inform and guide individualized treatment decisions for *P. aeruginosa* infections (6, 7, 9).

While six genes were found to be mutated independently by at least three evolved strains, these mutations were not clearly linked to resistance patterns (Fig. 5). This reflects prior reports of overall lower mutation frequency in *P. aeruginosa*, underpinning that phenotypic variability may play a stronger role in the development of antibiotic resistance than adaptive mutations (52). Consistent with previous reports on high transcriptional heterogeneity in *P. aeruginosa* clinical isolates (52, 53), we observed that the parental strain was the main driver of the transcriptional and proteomic profiles regardless of the antibiotic exposure.

Despite heterogeneous responses, machine learning approaches have previously been successful at predicting antibiotic resistance or virulence of clinical isolates based on genome or transcriptome features (34, 54, 55). Gene expression was more informative than mutation information for predicting resistance to meropenem and ceftazidime in *P. aeruginosa* (34). While our study's small sample size limits building generalizable machine learning models, PLS-DA's feature importance analysis helped us to identify candidate genes and proteins associated with resistance. Though potentially reflecting general drug stress response rather than direct resistance mechanisms, the identified genes and proteins could still serve as resistance and virulence biomarkers and inform combination treatments to suppress bacterial adaptation mechanisms and reduce antibiotic resistance.

The main categories of genes and proteins associated with antibiotic exposure include expected antibiotic resistance mechanisms such as membrane proteins, efflux pumps, and penicillin-binding proteins, as well as a large group of metabolic genes involved in energy production and lipopolysaccharide metabolism. Energy metabolism was mostly downregulated, likely reflecting stress-induced reduced bacterial metabolism. Conversely, lipopolysaccharide metabolism genes were generally upregulated, including those involved in alginate (PA0764 [*mucB*], PA0460) and lipid A biosynthesis (PA3552 [*arnB*], PA3554 [*arnA*]). Increased expression of *arnA/B* genes, along with mutations in their regulator *phoQ*, are linked to resistance against polymyxin antibiotics and antimicrobial peptides (56–58), and overexpression of *arnA* and *arnB* was observed to be more common among *P. aeruginosa* isolates resistant to CZA, when compared to other anti-pseudomonal antibiotics (35). Similarly, increased expression of alginate exopolysaccharide biosynthesis was previously observed in antibiotic-resistant strains isolated from a cystic fibrosis patient (53), and also appeared predictive of ceftazidime or ciprofloxacin resistance in machine learning models (34, 59). Since alginate production affects biofilm growth and decreases clearance by the host immune response (53), targeting alginate biosynthesis may be a strategy to complement antibiotic therapy.

The *mexAB-oprM* efflux system was preferentially upregulated in MEM-exposed strains. This system is regulated by the transcriptional repressors *mexR* and *nalD*, with additional indirect influence from *nalC* (60). Loss-of-function mutations in *mexR* and *nalD* are linked to increased resistance or elevated MICs to CZA (24, 35). In our assays, *nalD* mutations appeared in two MEM-exposed strains with significant upregulation of *mexA*, *mexB*, and *oprM*; however, these genes were also upregulated in three other strains with *nalD* downregulation, indicating that *nalD* mutations are not the sole mechanism modulating the *mexAB-oprM* efflux system. Additionally, mutations in *oprD*, encoding the outer membrane porin *oprD*, resulted in substantial downregulation of this gene and were observed exclusively in MEM-exposed strains, further highlighting its role in carbapenem resistance (61).

In contrast, significant upregulation of *ampC* was primarily observed in strains exposed to CZA, suggesting that this antibiotic induces the cephalosporinase. Mutations in *dacB*, encoding penicillin-binding protein PBP4 and implicated in *ampC* derepression via *ampR* (30, 58), were also found exclusively in CZA-selected strains.

A recent study detected AmpC overexpression in many of the isolates resistant to CZA (62). Mushtaq et al. (63) evaluated the role of *ampC* derepression in CZA resistance using 26 *Pseudomonas aeruginosa* strains with *ampC* mutations. Their findings showed that avibactam effectively reversed high-level ceftazidime resistance mediated by *ampC*, significantly reducing MICs in fully derepressed mutants. However, one strain with both high-level efflux activity and *ampC* derepression exhibited persistent resistance, highlighting the combined impact of efflux and *ampC* mutations on CZA resistance.

In our follow-up experiments with transposon insertion mutants in the *P. aeruginosa* mPAO1 strain, only 2 out of 15 mutants showed significant resistance changes, with CZA MIC decreasing by 25% or increasing up to threefold, though five other mutations were previously linked to altered resistance against various antibiotics (64) (Table S16). Since transposon insertions may not replicate changes seen in evolved clinical isolates, this could explain the assay's inability to reproduce resistance phenotypes.

To precisely address mutations found in genes associated with beta-lactam resistance, we performed CRISPR-Cas9 genome editing of four of the mutated genes: *dacB*, *ampC*, *mexB*, and *mexR*.

Mutations in *ampC* have been shown to enhance the ability of *ampC* to break down ceftazidime and to evade inhibition by avibactam more effectively (62). The introduction of a deletion within the *ampC*, identified in one of our strains that exhibited high resistance to CZA, resulted in only a slight increase in the CZA MIC level.

Previous studies identified a G115S mutation in *dacB* linked to *ampC* derepression (30), but its role in CZA resistance was unclear. While mutations slightly increased resistance overall, the most notable change was induced by a mutation in *dacB*, resulting in a fourfold increase in CZA MIC levels, though all MICs remained below the clinically relevant threshold of MIC >8 mg/L. These results underline that antibiotic resistance mechanisms involve complex interactions beyond single-gene effects, emphasizing the need for a systems-level approach to understand their multifaceted nature.

Cloning experiments revealed that introducing a wild-type copy of the *ampD* gene had the most pronounced effect on restoring CZA sensitivity to mutant strains—highlighting its key role in acquiring CZA resistance. However, attempts to introduce mutations via CRISPR-Cas9 were unsuccessful despite several efforts; cloning served as an alternative approach but exaggerated *ampD*'s effect due to overexpression from high-copy vectors like pUCP24 (60) compared to chromosomally encoded *ampD*. Editing through CRISPR-Cas9, by contrast, would better reflect bacterial physiology because this approach enables modification of the endogenous *ampD* gene to be done in a precise manner that maintains native expression levels and regulatory control, thus more closely mimicking natural genetic variations in bacterial populations.

Together with previous reports, this study emphasizes the importance of comprehensive sampling and multi-omics analyses for identifying biomarkers associated with

antibiotic resistance and informing combination therapies designed to suppress its evolution in clinical isolates of *P. aeruginosa*.

MATERIALS AND METHODS

Bacterial isolates and culture conditions

Eight clinical isolates of *Pseudomonas aeruginosa* were obtained from Kantonsspital St. Gallen in Switzerland. The isolates were sourced from three different clinical sites, namely urine ($n = 4$), sputum ($n = 3$), and blood culture ($n = 1$). For the multistep resistance selection process, bacterial cells were cultured in Luria Bertani (LB) broth using Nunc CELLSTAR six-well plates (Greiner Bio-One GmbH, Frickenhausen, Germany). The cultures were maintained with shaking at 120 rpm on a microplate shaker (Edmund Bühler GmbH, Germany) at a temperature of 37°C.

Ceftazidime-avibactam (Zavicefta, Pfizer) and meropenem (Meronem, Pfizer) were procured from our hospital pharmacy at Kantonsspital St. Gallen. Antibiotic stock solutions were prepared by dissolving powder stocks in accordance with the manufacturer's instructions. These solutions were then filter-sterilized through a 0.2 µm filter and stored at -20°C until used.

MIC determination/antimicrobial susceptibility testing

MICs for several antibiotics were determined by broth microdilution in Mueller–Hinton broth (MHB) using the Sensititre GNX2F plates (Thermo Fisher Scientific, East Grinstead, UK). MICs for MEM and CZA were further determined by Etest strips (bioMérieux, Chemin de l'Orme, France) and broth microdilution method (Table S4).

MICs for ceftolozane-tazobactam were determined by broth microdilution in MHB using ComASP Ceftolozane-tazobactam (Liofilchem, Brunschwig, Basel, Switzerland) and by Etest (bioMérieux, Chemin de l'Orme, France). The MIC determination adhered to the latest EUCAST recommendations (65), with values interpreted in accordance with the 2022 EUCAST criteria (version 12.0).

Evolution for antimicrobial resistance (multistep resistance selection)

Eight representative strains were selected from each of the original eight *Pseudomonas aeruginosa* isolates. This process involved isolating a single colony-forming unit (CFU), which was subsequently streaked onto a fresh MH agar plate. From each of these plates, three distinct colonies were carefully chosen to serve as parental strains for subsequent passage experiments. This resulted in 24 strains being passaged in each of the antibiotics (24 strains in CZA, 24 strains in MEM). For each individual strain, separate MIC measurements were conducted for CZA and MEM. To initiate the experiments, a single colony of each strain was selected after overnight growth at 37°C on an MH agar plate. Subsequently, each chosen colony was grown in 5 mL of LB broth at 37°C for 18 h without the presence of antibiotics (overnight culture). The strains were then concurrently exposed to sub-inhibitory concentrations, equivalent to one-fourth of the MIC values for each respective strain, of either CZA ($n = 3$) or MEM ($n = 3$). In brief, 5 mL of LB broth containing the corresponding antibiotic at a concentration of one-fourth of the MIC was inoculated with 25 µL of the overnight broth. The cultures were then agitated on a shaker under the previously described conditions, maintained at 37°C for a duration of 24 h. Subsequently, a daily transfer of 25 µL from the overnight culture was made to new LB broth containing CZA or MEM concentrations corresponding to one-fourth of the measured MIC. Following 6 consecutive days under the consistent influence of the same antibiotic concentration, the MICs were reassessed using the Etest. Based on the outcomes of these re-evaluated MICs, modifications were implemented to the antibiotic concentration for the subsequent cycle of passage.

Aliquots of 50 µL of the bacterial cultures were sampled after every six passages and kept in 1 mL 10% glycerol at -80°C for further molecular investigations. Furthermore,

a subset of strains was chosen at random and underwent matrix-assisted laser desorption/ionization time-of-flight analysis to ensure the absence of contaminants. To thoroughly assess the trajectory of resistance development and cross-resistance, the aforementioned protocol was replicated over a total of 18 sequential days. To comprehensively investigate the molecular mechanisms underlying resistance, those specific strains that had not exceeded the clinical breakpoint defined for each respective antibiotic, as specified by the EUCAST guidelines (66), underwent additional exposure to sub-inhibitory concentrations of the corresponding antibiotics. This exposure was continued until the strains developed resistance or for a maximum of 42 days. Concurrently, an identical procedure was conducted in the absence of antibiotic pressure, serving as negative controls for comparison.

Whole-genome sequencing

DNA extractions were conducted following the protocols outlined in the handbooks of two distinct kits: the QIAamp DNA Mini Kit (QIAGEN, Hilden, Germany) was employed for Illumina sequencing, while the QIAGEN Genomic-tip 100/G + Genomic DNA Buffer Set (QIAGEN, Hilden, Germany) kits were used for the parental strains that underwent PacBio sequencing. Whole-genome sequencing was carried out by Novogene (Cambridge, UK) and the Genomics Facility of the Department of Biosystems Science and Engineering of ETH Zürich (Basel, Switzerland).

For PacBio sequencing, a 10 kb SMRTbell library was prepared using the SMRTbell Template Prep Kit 1.0-SPv3 (Pacific Biosciences of California, USA). The qualified high-molecular-weight DNA was fragmented to approximately 10 kb, followed by processes such as damage repair, end repair, and adapter ligation. Subsequently, size selection was accomplished using a size-selection system.

The SMRTbell-Polymerase Complex was prepared utilizing the Sequel Binding Kit 2.0 (Pacific Biosciences of California, USA) and subsequently subjected to sequencing on a Sequel SMRT Cell (Pacific Biosciences of California, USA).

For Illumina sequencing, DNA samples were processed for library preparation following the manufacturer's recommendations of the NEBNext DNA Library Prep Kit (New England BioLabs, USA). Index codes were incorporated for each sample. In summary, genomic DNA was randomly fragmented to a size of 350 bp. The DNA fragments underwent end polishing, A-tailing, ligation with adapters, size selection, and further PCR enrichment. Subsequently, PCR products were purified using the AMPure XP system, their size distribution was assessed using the Agilent 2100 Bioanalyzer (Agilent Technologies, CA, USA), and quantification was performed using real-time PCR. The library was then sequenced on a NovaSeq 6000 S4 flow cell employing the PE150 strategy.

Mutation identification

Fasta files from the whole-genome sequencing were analyzed with the snippy perl package (version 4.6.0) (<https://github.com/tseemann/snippy>) to call the SNPs and other types of mutations using each parent strain genome sequenced before treatment as a reference. Other than options specifying the input files and output folder, snippy was called with default parameters and force and report flags and parallelized on 16 cores.

Sample preparation for transcriptomic profiling

The gene expression profiles of the resistant strains and the corresponding susceptible parent strains were analyzed with RNA sequencing involving three technical replicates for each condition. For RNA extraction, the RNeasy Protect Bacteria Reagent & RNeasy Mini kits (QIAGEN, Hilden, Germany) were utilized, following the RNeasy Protect Bacteria Reagent Handbook protocols 4 (Enzymatic Lysis and Proteinase K Digestion of Bacteria) and 7 (Purification of Total RNA from Bacterial Lysate Using the RNeasy Mini Kit). An optional on-column DNase digestion was performed using the RNeasy-Free DNase set (QIAGEN,

Hilden, Germany), and ribosomal RNA was depleted with the NEBNext rRNA Depletion Kit (New England BioLabs, Allschwil, Switzerland). The resulting RNA was fragmented, reverse transcribed, and prepared for sequencing on an Illumina NextSeq 500 platform. Sequencing comprised 150 bp single-end reads with a target of 5–10E6 reads per strain.

Protein extraction

Three milliliters of bacterial culture at an optical density (OD) of 1 was centrifuged to pellet the cells ($14,000 \times g$ for 5 min), washed 4× with 1× phosphate-buffered saline (PBS), and lysed with 100 μ L of buffer (4% [wt/vol] sodium dodecyl sulfate [SDS], 100 mM Tris/HCL, pH 8.2, 0.1 M DTT + phosphoSTOP [Roche Diagnostics GmbH, Mannheim, Germany]). One hundred microliters of lysis buffer (4% SDS in 50 mM triethylammonium bicarbonate buffer [TEAB]) was added to each sample. The samples were frozen in liquid nitrogen for 1 min and subsequently sonicated (sonication bath) for 2 min. These freeze/thaw cycles were repeated for a total of three times. For each sample, 12.5 units of Benzonase (Sigma-Aldrich) were added and the mixture was incubated for 15 minutes at room temperature while shaking at 700 rpm in an Eppendorf thermoshaker.

The samples were treated with high-intensity focused ultrasound (HIFU) for 1 min at an ultrasonic amplitude of 85% followed by further extraction using a tissue homogenizer (TissueLyser II, QIAGEN) for 4 min at 30 Hz. After another 1 min of HIFU, the samples were centrifuged at $20,000 \times g$ for 10 min.

The protein concentration was determined using a Lunatic (Unchained Labs) instrument. For each sample, 50 μ g of protein was taken and reduced with 2 mM TCEP (tris(2-carboxyethyl)phosphine) and alkylated with 15 mM iodoacetamide at 60°C for 30 min.

Protein digestion

The sp3 protein purification, digestion, and peptide clean-up were performed using a KingFisher Flex System (Thermo Fisher Scientific) and Carboxylate-Modified Magnetic Particles (GE Life Sciences) (67, 68). Beads were conditioned following the manufacturer's instructions, consisting of three washes with water at a concentration of 1 μ g/ μ L. Samples were diluted with an equal volume of 100% ethanol (50% ethanol final concentration). The beads, wash solutions, and samples were loaded into 96 deep well or microplates and transferred to the KingFisher.

The following steps were carried out on the robot: collection of beads from the last wash, protein binding to beads (14 min), washing of beads in wash solutions 1–3 (80% ethanol, 3 min each), protein digestion (offline from the KingFisher, overnight at RT with a trypsin:protein ratio of 1:50 in 50 mM TEAB), and peptide elution from the magnetic beads (water, 6 min). The digest solution and water elution were combined and dried to completeness. Afterwards, the peptides were re-dissolved in 40 μ L of 3% acetonitrile and 0.1% formic acid for MS analysis.

Proteomic analysis with liquid chromatography-mass spectrometry

Mass spectrometry (MS) analysis was performed on an Orbitrap Fusion Lumos (Thermo Scientific) equipped with a Digital PicoView source (New Objective) and coupled to a M-Class UPLC (Waters). The two channels had the following solvent compositions: channel A contained 0.1% formic acid, while channel B contained 0.1% formic acid and 99.9% acetonitrile. For each sample, 2 μ L of peptides was loaded on a commercial MZ Symmetry C18 Trap Column (100 \AA , 5 μ m, 180 μ m \times 20 mm, Waters) followed by nanoEase MZ C18 HSS T3 Column (100 \AA , 1.8 μ m, 75 μ m \times 250 mm, Waters). The peptides were eluted at a flow rate of 300 nL/min. After an initial hold at 5% B for 3 min, a gradient from 5 to 24% B in 80 min and 36% B in 10 min was applied. The column was washed with 95% B for 10 min and afterward, the column was re-equilibrated to starting conditions for an additional 10 min. Samples were acquired in a randomized order. The mass spectrometer was operated in data-dependent mode (DDA) acquiring

a full-scan MS spectrum (300–1,500 m/z) at a resolution of 120,000 at 200 m/z after accumulation to a target value of 500,000. Data-dependent MS/MS was recorded in the linear ion trap using quadrupole isolation with a window of 0.8 Da and higher-energy collisional dissociation (HCD) fragmentation with 35% fragmentation energy. The ion trap was operated in rapid scan mode with a target value of 10,000 and a maximum injection time of 50 ms. Only precursors with intensity above 5,000 were selected for MS/MS, and the maximum cycle time was set to 3 s. Charge state screening was enabled. Singly, unassigned, and charge states higher than seven were rejected. Precursor masses previously selected for MS/MS measurement were excluded from further selection for 20 s, and the exclusion window was set at 10 ppm. The samples were acquired using internal lock mass calibration on m/z 371.1012 and 445.1200. The mass spectrometry proteomics data were handled using the local laboratory information management system (69).

Protein identification and label-free quantification

The acquired raw MS data were processed by MaxQuant (version 1.6.2.3), followed by protein identification using the integrated Andromeda search engine (70). Spectra were searched against a *Pseudomonas aeruginosa* reference proteome (version from 2021 to 01-12), concatenated to its decoyed fasta database and common protein contaminants. Carbamidomethylation of cysteine was set as a fixed modification, while methionine oxidation and N-terminal protein acetylation were set as variable. Enzyme specificity was set to trypsin/P, allowing a minimal peptide length of seven amino acids and a maximum of two missed cleavages. MaxQuant Orbitrap default search settings were used. The maximum FDR was set to 0.01 for peptides and 0.05 for proteins. Label-free quantification was enabled, and a 2 min window for match between runs was applied. In the MaxQuant experimental design template, each file is kept separate in the experimental design to obtain individual quantitative values. Protein fold changes were computed based on intensity values reported in the proteinGroups.txt file. The proteinGroups.txt file generated by MaxQuant was used for downstream analysis to compute a moderated t -test (71) for all proteins quantified with at least two peptides employing the R package limma (72). Protein abundances were normalized using quantile normalization. A set of functions implemented in the R package SRMSservice (73) was used to filter for proteins with two or more peptides allowing for a maximum of four missing values, to normalize the data with a modified robust z -score transformation, and to compute P -values using the t -test with pooled variance. If all measurements of a protein are missing in one of the conditions, a pseudo fold change was computed, replacing the missing group average by the mean of 10% smallest protein intensities in that condition.

Transcriptomics data analysis

Quantification of transcriptomic data were performed by using Trimmomatic (version 0.39) (74) followed by Salmon (version 1.10.1) (75) packages. DESeq2 (version 1.38.0) (76) R package was used to perform normalization and differential expression analysis, first by importing the data generated by the Salmon package using the tximport R package (version 1.26.0) (77), then by running DESeqDataSetFromTximport and DESeq functions. The aforementioned tools were run on all samples using a Snakemake pipeline (78). Differential analysis was performed for each strain comparing expression levels in each evolved strain (on CZA and MEM) to the parent strain expression, as well as between CZA- and MEM-evolved strains of the same parent. Furthermore, to filter the results from PLS-DA feature importance analysis, all the strains were grouped based on their MEM- or CZA-resistance levels with the threshold of MIC = 32 mg/L indicating high resistance. Differential analysis was performed between all sensitive versus resistant strains for each antibiotic (for MEM: all parent strains and CZA-exposed 2_C, 3_C, 4_C, 5_B, and 6_C strains versus CZA-exposed 1_B and all MEM-exposed strains; for CZA: all parent strains, CZA-exposed 3_C and 6_C and MEM-exposed 2_C, 3_C, 4_C, and 5_B versus CZA-exposed 1_B, 2_C, 4_C, 5_B and MEM-exposed 1_B and 6_C strains), as well as all sensitive versus resistant

exposed to the same antibiotic (for MEM: CZA-exposed 2_C, 3_C, 4_C, 5_B, and 6_C strains versus CZA-exposed 1_B strain; for CZA: CZA-exposed 3_C and 6_C versus CZA-exposed 1_B, 2_C, 4_C, and 5_B strains, or MEM-exposed 2_C, 3_C, 4_C, and 5_B strains versus MEM-exposed 1_B and 6_C strains). DESeq2 utilizes Wald test to compare expression levels between conditions with Benjamini-Hochberg correction for multiple hypothesis testing. All the processing of the data were executed on the EMBL Heidelberg HPC cluster (79).

Partial least squares discriminant analysis

PLS-DA was performed by using the function PLSRegression from the scikit-learn python package (version 1.3.0) to predict whether CZA or MEM resistance was high (1) or low (0). Threshold of MIC = 32 mg/L was used to define high resistance. First set of models used all of the transcriptomic and proteomic data for fitting ($n = 51$ samples) to determine the separation of samples with high and low MIC values in the lower dimensional space. The second set of models used a leave-one-strain-out strategy—data related to one of the strains left out of the training set ($n = 6$ – 9 samples), then these data were used as a test set to determine the accuracy of the predictions for the model trained on all the other strains ($n = 42$ – 45 samples). To determine a set of the most important features (genes or proteins) contributing to the separation of the samples with high and low MIC values, the top 100 features by absolute values of weights were selected from each leave-one-strain-out model for the first and the second PLS factor (200 features per model in total).

Gene ontology enrichment analysis

Gene ontology terms were determined by querying PantherDB REST API (<https://pantherdb.org/services/oai/pantherdb/enrich/overrep>) with a set of genes or proteins that resulted from differential expression and differential abundance analyses and PLS-DA analysis. Significantly upregulated or downregulated [FDR < 0.05 and $\text{abs}(\log_2\text{FC}) > 1$] genes and proteins from differential expression and differential abundance analyses were passed to the PantherDB to perform over-representation analysis. Similarly, genes and proteins determined by PLS-DA as contributing to the top 200 weights of leave-one-strain-out models and appearing in at least five models were passed to the PantherDB API. Over-representation analysis done by the PantherDB service assumes that all *P. aeruginosa* genes are present in the reference list.

Sequence typing and phylogenetic analysis

To have the genetic background of the strains in this study compared with each other and with genomes of other publicly available strains, sequence typing analysis and phylogenetic analysis were performed. Sequence typing was performed using the PubMLST web service (<https://pubmlst.org>) (80). Phylogenetic analysis was performed using Mashtree (version 1.4.6) (81), first comparing just the strains in this study, then comparing them to strains with complete genomes available from a database of pseudomonas genomes (<https://pseudomonas.com>) (82) and matplotlib (version 3.8.3) (83).

Comparison to public data sets

Several publicly available data sets were used for comparison with the results of the differential expression analysis conducted in this study. Dong et al. (32) data set (32) was processed from raw reads with the same pipeline as for the data set in this study, specifically by using Salmon (version 1.10.1) (75) followed by DESeq2 (version 1.38.0) (76). Khaledi et al. (34) data set, consisting of a counts table, was processed with DESeq2 as well, by running DESeqDataSetFromMatrix and then DESeq functions. Additionally, two data sets, Alam (84) and Castanheira (35), had already undergone differential expression analysis. Significantly upregulated or downregulated genes from each data set were compared with those from this study on a per-strain basis. This comparison was

performed by calculating the ratio of the size of the intersection of two given sets to the size of each set and applying Fisher's exact test to the intersection. *P*-values were subsequently adjusted with the Benjamini-Hochberg procedure.

Data selection and visualization for the summary plot

A data-driven approach was employed to select the genes and proteins shown in Fig. 5 from mutation analysis, differential analysis, and PLS-DA. From mutation analysis, genes with mutations present in at least two strains were selected. From differential analysis, genes and proteins significantly upregulated or downregulated [$\text{abs}[\log_2(\text{fold change})] \geq 1$ in either of the omics, $\text{FDR} < 0.05$ in both omics] by at least five strains from transcriptomics, four strains from proteomics, and three strains from both were selected. From PLS-DA, genes and proteins that appear in the top 200 features in at least five leave-one-strain-out models and additionally significantly differentially abundant between the groups of sensitive and resistant strains (see section Transcriptomics data analysis for details) were selected. The grouping of the final list of genes and proteins, obtained by combining these sets of genes and proteins, was performed by ChatGPT by providing the list of locus tags and using the prompt "can you group the following list of genes based on their functions" followed by manual checks and corrections.

MIC measurement of the selected mutant strains of *P. aeruginosa* mPAO1

P. aeruginosa mPAO1 parent strain and its transposon insertion mutants were obtained from the *P. aeruginosa* Two-Allele Library of the Manoil Lab (85). Bacteria were activated on plate count agar (Sigma Aldrich, Steinheim, Germany). Single colonies from the plates were picked up and inoculated in 25 mL MHB (Sigma Aldrich, Steinheim, Germany) and cultivated overnight at 37°C and 160 rpm. A total of 250 μL of the overnight culture was added to 25 mL MHB and further incubated for 3 h to obtain the exponentially growing cells. The final culture was diluted to an OD of 0.1 measured at 600 nm, which corresponds to approximately 10^8 CFU/mL, of which 500 μL was transferred to 50 mL MHB and mixed well by vortexing. Antibiotic stock solutions for MEM were prepared as mentioned above. CZA for micro broth dilution was prepared with ceftazidime (Sigma Aldrich, Steinheim, Germany) and avibactam (Sigma Aldrich, Steinheim, Germany), the latter with a fixed concentration of 4 mg/L per well.

The MIC assays of the MEM and CZA were performed in 96-well plates (BRAND microplate BRANDplates, Sigma Aldrich, Steinheim, Germany) covered with an air-permeable foil (Breathe-Easy sealing membrane Sigma Aldrich, Steinheim, Germany) and incubated at 37°C without shaking. All assays were done in MHB medium supplemented with increasing concentrations of antibiotics and inoculated with mPAO1 mutants of 5×10^5 CFU/mL. For each condition, four replicates were included. After 24 h at 37°C, the bacterial growth was measured at OD 600 nm.

Cloning of *ampD* gene in the evolved CZA-resistant strain

The wild-type *ampD* allele was amplified from the parental 2c isolate using primers *ampD*-Fw (5'-GATGATGAGCTCGCGCCGCTGGATTAGAGT-3') and *ampD*-Rev (5'-GATGATGATCCAGCAGCAACACCAGGAAC-3'), and cloned into vector pUCP24, before transformation into *E. coli* Top10. Transformants were selected on plates supplemented with gentamicin (25 mg/L). Successful transformants were confirmed by PCR amplification and sequencing of the alleles, then transformed into the parent and the CZA-evolved mutant 2c strains. Susceptibility testing was performed by disk diffusion, and MICs were determined by broth microdilution according to EUCAST guidelines.

CRISPR-Cas9 genome editing

CRISPR-Cas9 genome editing was performed using the two-plasmid (pCasPA/pACRISPR) method developed by Chen et al. (86) using the λ -Red recombination system.

Single guide RNA (sgRNA) oligos were designed with CRISPOR (87) and the overhangs added according to Table S16.

Oligos were phosphorylated and annealed by mixing 35 μ L H₂O, 5 μ L 10 \times T4 Polynucleotide Kinase Buffer (New England BioLabs, Ipswich, MA, USA), 5 μ L fresh 10 mM ATP, 1 μ L T4 polynucleotide kinase (New England BioLabs, Ipswich, MA, USA), and 2 μ L of each oligo (50 μ M). After 1 h of incubation at 37°C, 2.5 μ L 1 M NaCl was added, and the mix was heated to 95°C for 3 min and then cooled to 25°C by decreasing the temperature -0.1°C per second. The annealed oligos were diluted 1:20. Then, 1 μ L of the diluted oligos was combined with 1.5 μ L of H₂O, 5 μ L of 2 \times Quick Ligase Buffer (NEB), 20 nM pACRISPR plasmid, 0.5 μ L Quick Ligase (400 U/ μ L), 0.5 μ L BsaI-HFv2 (NEB), and 0.5 μ L fresh 10 mM ATP. The reaction mixture was then placed in a thermocycler for 25 cycles of 37°C for 3 minutes and 16°C for 4 minutes. Afterwards, the mixture was incubated at 80°C for 15 minutes and finally cooled down to 10°C. The product was transformed into Zymo Mix & Go (Takara, Mountain View, CA, USA) competent *E. coli* and selected on 50 mg/L carbenicillin plates. Insertion of the sgRNA sequence was verified by sequencing (sgSeq-F primer). Primers for the repair of 500 bp arms were designed with the Takara In-Fusion Cloning Primer Design Tool to contain the desired restriction sites and the desired nucleotide change and a synonymous change of the protospacer adjacent motif (PAM) sequence. Repair arms were inserted in between the XhoI and XbaI restriction sites of the pACRISPR plasmid following the Takara In-Fusion PCR Cloning systems protocol, and insertion was verified by PCR and sequencing. *P. aeruginosa* mPAO1 was made electrocompetent by diluting an overnight culture 1:100 in fresh lysogeny broth (LB) and incubating them at 37°C until OD₆₀₀ of ~ 0.5 . Cells were chilled on ice for 30 min, then were harvested by centrifugation at 3,300 rpm for 5 min, pellet washed twice with 20 mL of ice-cold 10% glycerol, and then resuspended in 1 mL 10% glycerol. A total of 50 μ L electrocompetent cells was mixed with up to 5 μ L of pCas plasmid and electroporated in a 1 mm cuvette (1.8 kV, 200 Ω , 25 μ F). Immediately after the pulse, 1 mL LBB was added, and the mix was incubated for 90 min at 37°C, 200 rpm followed by selection on 30 mg/L tetracycline plates.

Afterward, one colony harboring the pCasPA plasmid was prepared as electrocompetent cells, same as above except for the addition of 2 mg/L total concentration L-arabinose at OD 0.3. pACRISPR with the sgRNA sequence and repair arms were mixed, and electroporation followed with the same conditions. A total of 30 mg/L tetracycline and 100 mg/L carbenicillin were used for selection.

Transformants were plasmid-cured by growing them in the absence of antibiotics until evident growth and then plating a 1:10⁴ dilution on 5% sucrose LB agar. The PCR-amplified region of the CRISPR site of plasmid-cured bacteria was sequenced to confirm the CRISPR event.

ACKNOWLEDGMENTS

We thank the members of the Zimmermann-Kogadeeva lab for helpful discussions; the Functional Genomics Center Zurich for technical assistance with proteomics measurements, Stefanie Altenried and Flavia Zuber at Empa for their assistance with analyzing the mPAO1 insertion mutants, Valentin Gisler from Cantonal Hospital Aarau for providing clinical isolates, and the Genomics Facility Basel (Department of Biosystems Science and Engineering, ETH Zürich) for WGS and RNAseq analysis. We also thank the EMBL IT Services staff for managing and provision of access to the HPC resources.

The work was supported by the European Molecular Biology Laboratory (B.J.B. and M.Z.-K.) and through a grant from the Research Committee of the Kantonsspital St.Gallen (B.B.F.).

Study and experiment design: B.B.F. and M.Z.-K. Data analysis: B.J.B., S.S., M.Z.-K., A.B. *In vitro* experiments: A.B., J.F., Q.R., N.R.I.. Clinical isolate work: A.B., B.B.F., A.E. Manuscript writing: B.J.B., M.Z.-K., B.B.F., A.B. Manuscript editing: B.J.B., A.B., S.S., N.R.I., Q.R., J.F., A.E., M.Z.-K., B.B.F. Funding acquisition: B.B.F., M.Z.-K. All authors read and approved the manuscript.

In the preparation of this research paper, we utilised generative AI tools (ChatGPT 4o and perplexity.ai) to enhance the clarity and coherence of our writing, including this section. We carefully reviewed and edited the AI-generated recommendations to maintain the integrity and authenticity of our work. Generative AI tools were not used to produce new content, but only to rephrase human-written text to improve its clarity. ChatGPT 4o was also used to suggest the clustering of genes based on their functions in Fig. 5 (described in Materials and Methods), which was subsequently edited by the authors.

AUTHOR AFFILIATIONS

¹Genome Biology Unit, European Molecular Biology Laboratory, Heidelberg, Germany

²HOCH, Cantonal Hospital St. Gallen, Medical Research Center, St. Gallen, Switzerland

³HOCH, Division of Infectious Diseases, Infection Prevention and Travel Medicine, Cantonal Hospital St. Gallen, St. Gallen, Switzerland

⁴Department of Biosystems Science and Engineering, ETH Zürich, Basel, Switzerland

⁵Graduate School for Cellular and Biomedical Sciences, University of Bern, Bern, Switzerland

⁶Empa, Swiss Federal Laboratories for Materials Science and Technology, St. Gallen, Switzerland

⁷Medical and Molecular Microbiology, Faculty of Science and Medicine, University of Fribourg, Fribourg, Switzerland

⁸Institute of Medical Microbiology, University of Zürich, Zürich, Switzerland

⁹Department of Infectious Diseases, Inselspital, Bern University Hospital, University of Bern, Bern, Switzerland

AUTHOR ORCIDs

Bartosz J. Bartmanski  <http://orcid.org/0000-0002-0495-9150>

Qun Ren  <http://orcid.org/0000-0003-0627-761X>

Jacqueline Findlay  <http://orcid.org/0000-0002-7335-9001>

Adrian Egli  <http://orcid.org/0000-0002-3564-8603>

Maria Zimmermann-Kogadeeva  <http://orcid.org/0000-0001-6021-1246>

Baharak Babouee Flury  <http://orcid.org/0000-0001-8966-5882>

FUNDING

Funder	Grant(s)	Author(s)
European Molecular Biology Laboratory		Maria Zimmermann-Kogadeeva Bartosz J. Bartmanski
Research Committee of Cantonal Hospital St. Gallen		Baharak Babouee Flury

AUTHOR CONTRIBUTIONS

Bartosz J. Bartmanski, Data curation, Formal analysis, Investigation, Software, Writing – original draft, Writing – review and editing | Anja Bösch, Formal analysis, Investigation, Writing – review and editing | Steven Schmitt, Formal analysis | Niranjan R. Ireddy, Investigation, Writing – review and editing | Qun Ren, Investigation, Writing – review and editing | Jacqueline Findlay, Investigation, Writing – review and editing | Adrian Egli, Resources, Writing – review and editing | Maria Zimmermann-Kogadeeva, Conceptualization, Formal analysis, Funding acquisition, Investigation, Writing – original draft, Writing – review and editing | Baharak Babouee Flury, Conceptualization, Funding acquisition, Methodology, Writing – original draft, Writing – review and editing

DATA AVAILABILITY

The genomics and transcriptomics data have been deposited in the European Nucleotide Archive (ENA) repository <https://www.ebi.ac.uk/ena/browser/view/PRJEB76120>. Proteomics data have been deposited to the ProteomeXchange Consortium via the PRIDE (<http://www.ebi.ac.uk/pride>) repository with the data set identifier PXD044998. Supplemental tables and supporting data are available in the following Zenodo archive: <https://zenodo.org/uploads/15235346>. Code to reproduce all the analysis in this work can be found in the following git repository: <https://git.embl.de/grp-zimmermann-koga-deeva/PseudomonasAntibioticsResistance>.

ADDITIONAL FILES

The following material is available [online](#).

Supplemental Material

Supplemental tables, part 1 (mBio03896-24-s0001.xlsx). Tables S1 to S5, S6ab, and S7ab.

Supplemental tables, part 2 (mBio03896-24-s0002.xlsx). Tables S9 to S16

Supplemental material (mBio03896-24-s0003.docx). Figures S1 to S9 and Table S17.

Table S6c, part 1 (mBio03896-24-s0004.xlsx). CZA vs PAR comparison

Table S6c, part 2 (mBio03896-24-s0005.xlsx). MEM vs PAR comparison.

Table S6c, part 3 (mBio03896-24-s0006.xlsx). CZA vs MEM comparison.

Table S7c (mBio03896-24-s0007.xlsx). Fold changes and *P*-values for all detected proteins.

Table S8a (mBio03896-24-s0008.xlsx). Gene ontology enrichment results for differentially expressed genes and proteins.

Table S8bc (mBio03896-24-s0009.xlsx). Additional gene ontology enrichment results.

REFERENCES

- Cabot G, Zamorano L, Moyà B, Juan C, Navas A, Blázquez J, Oliver A. 2016. Evolution of *Pseudomonas aeruginosa* antimicrobial resistance and fitness under low and high mutation rates. *Antimicrob Agents Chemother* 60:1767–1778. <https://doi.org/10.1128/AAC.02676-15>
- Gellatly SL, Hancock REW. 2013. *Pseudomonas aeruginosa*: new insights into pathogenesis and host defenses. *Pathog Dis* 67:159–173. <https://doi.org/10.1111/2049-632X.12033>
- Pang Z, Raudonis R, Glick BR, Lin TJ, Cheng Z. 2019. Antibiotic resistance in *Pseudomonas aeruginosa*: mechanisms and alternative therapeutic strategies. *Biotechnol Adv* 37:177–192. <https://doi.org/10.1016/j.biotechadv.2018.11.013>
- Carmeli Y, Troillet N, Eliopoulos GM, Samore MH. 1999. Emergence of antibiotic-resistant *Pseudomonas aeruginosa*: comparison of risks associated with different antipseudomonal agents. *Antimicrob Agents Chemother* 43:1379–1382. <https://doi.org/10.1128/AAC.43.6.1379>
- Cohen NR, Lobritz MA, Collins JJ. 2013. Microbial persistence and the road to drug resistance. *Cell Host Microbe* 13:632–642. <https://doi.org/10.1016/j.chom.2013.05.009>
- Ambreetha S, Zincke D, Balachandar D, Mathee K. 2024. Genomic and metabolic versatility of *Pseudomonas aeruginosa* contributes to its interkingdom transmission and survival. *J Med Microbiol* 73:001791. <https://doi.org/10.1099/jmm.0.001791>
- Livermore DM. 2002. Multiple mechanisms of antimicrobial resistance in *Pseudomonas aeruginosa*: our worst nightmare? *Clin Infect Dis* 34:634–640. <https://doi.org/10.1086/338782>
- Reynolds D, Kollef M. 2021. The epidemiology and pathogenesis and treatment of *Pseudomonas aeruginosa* infections: an update. *Drugs (Abingdon)* 81:2117–2131. <https://doi.org/10.1007/s40265-021-01635-6>
- Chamot E, Boffi El Amari E, Rohner P, Van Delden C. 2003. Effectiveness of combination antimicrobial therapy for *Pseudomonas aeruginosa* bacteremia. *Antimicrob Agents Chemother* 47:2756–2764. <https://doi.org/10.1128/AAC.47.9.2756-2764.2003>
- O'Callaghan CH, Acred P, Harper PB, Ryan DM, Kirby SM, Harding SM. 1980. GR 20263, a new broad-spectrum cephalosporin with anti-pseudomonal activity. *Antimicrob Agents Chemother* 17:876–883. <https://doi.org/10.1128/AAC.17.5.876>
- Farra A, Islam S, Strålfors A, Sörberg M, Wretling B. 2008. Role of outer membrane protein OprD and penicillin-binding proteins in resistance of *Pseudomonas aeruginosa* to imipenem and meropenem. *Int J Antimicrob Agents* 31:427–433. <https://doi.org/10.1016/j.ijantimicag.2007.12.016>
- Riera E, Cabot G, Mulet X, García-Castillo M, del Campo R, Juan C, Cantón R, Oliver A. 2011. *Pseudomonas aeruginosa* carbapenem resistance mechanisms in Spain: impact on the activity of imipenem, meropenem and doripenem. *J Antimicrob Chemother* 66:2022–2027. <https://doi.org/10.1093/jac/dkr232>
- Shu J-C, Kuo A-J, Su L-H, Liu T-P, Lee M-H, Su I-N, Wu T-L. 2017. Development of carbapenem resistance in *Pseudomonas aeruginosa* is associated with OprD polymorphisms, particularly the amino acid substitution at codon 170. *J Antimicrob Chemother* 72:2489–2495. <https://doi.org/10.1093/jac/dkx158>
- Drawz SM, Bonomo RA. 2010. Three decades of beta-lactamase inhibitors. *Clin Microbiol Rev* 23:160–201. <https://doi.org/10.1128/CMR.00037-09>
- Shirley M. 2018. Ceftazidime-avibactam: a review in the treatment of serious gram-negative bacterial infections. *Drugs (Abingdon)* 78:675–692. <https://doi.org/10.1007/s40265-018-0902-x>
- Mushtaq S, Vickers A, Woodford N, Livermore DM. 2024. Activity of aztreonam/avibactam and ceftazidime/avibactam against Enterobacteriales with carbapenemase-independent carbapenem resistance. *Int J Antimicrob Agents* 63:107081. <https://doi.org/10.1016/j.ijantimicag.2023.107081>
- Humphries RM, Yang S, Hemarajata P, Ward KW, Hindler JA, Miller SA, Gregson A. 2015. First report of Ceftazidime-avibactam resistance in a KPC-3-expressing *Klebsiella pneumoniae* isolate. *Antimicrob Agents Chemother* 59:6605–6607. <https://doi.org/10.1128/AAC.01165-15>
- Sauerborn E, Corredor NC, Reska T, Perlas A, Vargas da Fonseca Atum S, Goldman N, Wantia N, Prazeres da Costa C, Foster-Nyarko E, Urban L. 2024. Detection of hidden antibiotic resistance through real-time

- genomics. *Nat Commun* 15:5494. <https://doi.org/10.1038/s41467-024-49851-4>
19. Lahiri SD, Walkup GK, Whiteaker JD, Palmer T, McCormack K, Tanudra MA, Nash TJ, Thresher J, Johnstone MR, Hajec L, Livchak S, McLaughlin RE, Alm RA. 2015. Selection and molecular characterization of ceftazidime/avibactam-resistant mutants in *Pseudomonas aeruginosa* strains containing derepressed AmpC. *J Antimicrob Chemother* 70:1650–1658. <https://doi.org/10.1093/jac/dkv004>
 20. Fraile-Ribot PA, Cabot G, Mulet X, Periañez L, Martín-Pena ML, Juan C, Pérez JL, Oliver A. 2018. Mechanisms leading to *in vivo* ceftolozane/tazobactam resistance development during the treatment of infections caused by MDR *Pseudomonas aeruginosa*. *J Antimicrob Chemother* 73:658–663. <https://doi.org/10.1093/jac/dkx424>
 21. Diaz-Cañestro M, Periañez L, Mulet X, Martín-Pena ML, Fraile-Ribot PA, Ayestarán I, Colomar A, Nuñez B, Maciá M, Novo A, Torres V, Asensio J, López-Causapé C, Delgado O, Pérez JL, Murillas J, Riera M, Oliver A. 2018. Ceftolozane/tazobactam for the treatment of multidrug resistant *Pseudomonas aeruginosa*: experience from the Balearic Islands. *Eur J Clin Microbiol Infect Dis* 37:2191–2200. <https://doi.org/10.1007/s10096-018-3361-0>
 22. Dos Santos BS, da Silva LCN, da Silva TD, Rodrigues JFS, Grisotto MAG, Correia MTDS, Napoleão TH, da Silva MV, Paiva PMG. 2016. Application of Omics Technologies for Evaluation of Antibacterial Mechanisms of Action of Plant-Derived Products. *Front Microbiol* 7:1466. <https://doi.org/10.3389/fmicb.2016.01466>
 23. Maity R, Zhang X, Liberati FR, Rossi CS, Cutruzzola F, Rinaldo S, et al. 2024. Merging multi-omics with proteome integral solubility alteration unveils antibiotic mode of action. *Elife* 13:RP96343. <https://doi.org/10.7554/eLife.96343.3>
 24. Chernov VM, Chernova OA, Mouzykantov AA, Lopukhov LL, Aminov RI. 2019. Omics of antimicrobials and antimicrobial resistance. *Expert Opin Drug Discov* 14:455–468. <https://doi.org/10.1080/17460441.2019.1588880>
 25. Molina-Mora JA, García F. 2021. Molecular determinants of antibiotic resistance in the costa rican *Pseudomonas aeruginosa* AG1 by a multi-omics approach: a review of 10 years of study. *Phenomics* 1:129–142. <https://doi.org/10.1007/s43657-021-00016-z>
 26. Jo S-H, Song W-S, Park H-G, Lee J-S, Jeon H-J, Lee Y-H, Kim W, Joo H-S, Yang Y-H, Kim J-S, Kim Y-G. 2020. Multi-omics based characterization of antibiotic response in clinical isogenic isolates of methicillin-susceptible/-resistant *Staphylococcus aureus* RSC Adv 10:27864–27873. <https://doi.org/10.1039/d0ra05407k>
 27. Khil PP, Dulanto Chiang A, Ho J, Youn J-H, Lemon JK, Gea-Banacloche J, Frank KM, Parta M, Bonomo RA, Dekker JP. 2019. Dynamic emergence of mismatch repair deficiency facilitates rapid evolution of ceftazidime-avibactam resistance in *Pseudomonas aeruginosa* acute infection. *mBio*:e01822-19. <https://doi.org/10.1128/mBio.01822-19>
 28. Castanheira M, Doyle TB, Smith CJ, Mendes RE, Sader HS. 2019. Combination of MexAB-OprM overexpression and mutations in efflux regulators, PBP3 and chaperone proteins is responsible for ceftazidime/avibactam resistance in *Pseudomonas aeruginosa* clinical isolates from US hospitals. *J Antimicrob Chemother* 74:2588–2595. <https://doi.org/10.1093/jac/dkz243>
 29. Babouee Flury B, Bösch A, Gislis V, Egli A, Seiffert SN, Nolte O, et al. 2023. Multifactorial resistance mechanisms associated with resistance to ceftazidime-avibactam in clinical *Pseudomonas aeruginosa* isolates from Switzerland. Available from: <https://www.frontiersin.org/articles/10.3389/fcimb.2023.1098944>
 30. Sanz-García F, Hernando-Amado S, Martínez JL. 2018. Mutation-driven evolution of *Pseudomonas aeruginosa* in the presence of either ceftazidime or ceftazidime-avibactam. *Antimicrob Agents Chemother* 62:01379–18. <https://doi.org/10.1128/AAC.01379-18>
 31. EUCAST. 2023. Breakpoint tables for interpretation of MICs and zone diameters. Available from: https://www.eucast.org/fileadmin/src/media/PDFs/EUCAST_files/Breakpoint_tables/v_12.0_Breakpoint_Tables.pdf. Retrieved 7 Dec 2023.
 32. Dong L, Sun L, Yang Y, Yuan L, Gao W, Yu D, Meng Q, Shi W, Wang Q, Li Y, Zhang Y, You X, Yao K. 2024. Non-antibiotic pharmaceutical phenylbutane binding to MexR reduces the antibiotic susceptibility of *Pseudomonas aeruginosa*. *Microbiol Res* 288:127872. <https://doi.org/10.1016/j.micres.2024.127872>
 33. Alam F, Blair JMA, Hall RA. 2023. Transcriptional profiling of *Pseudomonas aeruginosa* mature single- and dual-species biofilms in response to meropenem. *Microbiology (Reading)* 169:001271. <https://doi.org/10.1099/mic.0.001271>
 34. Khaledi G, Kolari A, Gastmeier P, Hogardt M, Jonas D, Mofrad MR, Bremges A, McHardy AC, Häussler S. 2020. Predicting antimicrobial resistance in *Pseudomonas aeruginosa* with machine learning-enabled molecular diagnostics. *EMBO Mol Med* 12:e10264. <https://doi.org/10.15252/emmm.201910264>
 35. Castanheira M, Doyle TB, Hubler CM, Collingsworth TD, DeVries S, Mendes RE. 2022. The plethora of resistance mechanisms in *Pseudomonas aeruginosa*: transcriptome analysis reveals a potential role of lipopolysaccharide pathway proteins to novel β -lactam/ β -lactamase inhibitor combinations. *J Glob Antimicrob Resist* 31:72–79. <https://doi.org/10.1016/j.jgar.2022.07.021>
 36. Ruiz-Perez D, Guan H, Madhivanan P, Mathee K, Narasimhan G. 2020. So you think you can PLS-DA? *BMC Bioinformatics* 21:2. <https://doi.org/10.1186/s12859-019-3310-7>
 37. Barker M, Rayens W. 2003. Partial least squares for discrimination. *J Chemom* 17:166–173. <https://doi.org/10.1002/cem.785>
 38. Maunders EA, Triniman RC, Western J, Rahman T, Welch M. 2020. Global reprogramming of virulence and antibiotic resistance in *Pseudomonas aeruginosa* by a single nucleotide polymorphism in elongation factor, *fusA1* *J Biol Chem* 295:16411–16426. <https://doi.org/10.1074/jbc.RA119.012102>
 39. Sindeldecke D, Stoodley P. 2021. The many antibiotic resistance and tolerance strategies of *Pseudomonas aeruginosa*. *Biofilm* 3:100056. <https://doi.org/10.1016/j.biofilm.2021.100056>
 40. Huse HK, Kwon T, Zlosnik JEA, Speert DP, Marcotte EM, Whiteley M, editor. 2013. *Pseudomonas aeruginosa* enhances production of a non-alginate exopolysaccharide during long-term colonization of the cystic fibrosis lung. *PLoS One* 8:e82621. <https://doi.org/10.1371/journal.pone.0082621>
 41. Scott NE, Hare NJ, White MY, Manos J, Cordwell SJ. 2013. Secretome of transmissible *Pseudomonas aeruginosa* AES-1R grown in a cystic fibrosis lung-like environment. *J Proteome Res* 12:5357–5369. <https://doi.org/10.1021/pr4007365>
 42. Woods EC, McBride SM. 2017. Regulation of antimicrobial resistance by extracytoplasmic function (ECF) sigma factors. *Microbes Infect* 19:238–248. <https://doi.org/10.1016/j.micinf.2017.01.007>
 43. Kong KF, Schnepfer L, Mathee K. 2010. Beta-lactam antibiotics: from antibiotic to resistance and bacteriology. *APMIS* 118:1–36. <https://doi.org/10.1111/j.1600-0463.2009.02563.x>
 44. Czub MP, Zhang B, Chiarelli MP, Majorek KA, Joe L, Porebski PJ, Revilla A, Wu W, Becker DP, Minor W, Kuhn ML. 2018. A Gcn5-related N-acetyltransferase (GNAT) capable of acetylating polymyxin B and colistin antibiotics *in vitro*. *Biochemistry* 57:7011–7020. <https://doi.org/10.1021/acs.biochem.8b00946>
 45. Sigurdsson G, Fleming RMT, Heinken A, Thiele I. 2012. A systems biology approach to drug targets in *Pseudomonas aeruginosa* biofilm. *PLoS One* 7:e34337. <https://doi.org/10.1371/journal.pone.0034337>
 46. Cirz RT, O'Neill BM, Hammond JA, Head SR, Romesberg FE. 2006. Defining the *Pseudomonas aeruginosa* SOS response and its role in the global response to the antibiotic ciprofloxacin. *J Bacteriol* 188:7101–7110. <https://doi.org/10.1128/JB.00807-06>
 47. Duang-Nkern J, Nontaleerak B, Thongphet A, Asano K, Chujan S, Satayavivad J, Sukchawalit R, Mongkolsuk S. 2024. Regulation of curcumin reductase curA (PA2197) through sodium hypochlorite and N-ethylmaleimide sensing by TetR family repressor CurR (PA2196) in *Pseudomonas aeruginosa*. *Gene* 927:148754. <https://doi.org/10.1016/j.gene.2024.148754>
 48. Ramos PIP, Fernández Do Porto D, Lanzarotti E, Sosa EJ, Burguener G, Pardo AM, Klein CC, Sagot M-F, de Vasconcelos ATR, Gales AC, Marti M, Turjanski AG, Nicolás MF. 2018. An integrative, multi-omics approach towards the prioritization of *Klebsiella pneumoniae* drug targets. *Sci Rep* 8:10755. <https://doi.org/10.1038/s41598-018-28916-7>
 49. Sobel ML, Hocquet D, Cao L, Plesiat P, Poole K. 2005. Mutations in PA3574 (nalD) lead to increased MexAB-OprM expression and multidrug resistance in laboratory and clinical isolates of *Pseudomonas aeruginosa*. *Antimicrob Agents Chemother* 49:1782–1786. <https://doi.org/10.1128/AAC.49.5.1782-1786.2005>
 50. Adewoye L, Sutherland A, Sri Kumar R, Poole K. 2002. The mexR repressor of the mexAB-oprM multidrug efflux operon in *Pseudomonas aeruginosa*: characterization of mutations compromising activity. *J Bacteriol* 184:4308–4312. <https://doi.org/10.1128/JB.184.15.4308-4312.2002>

51. Castanheira M, Kimbrough JH, Lindley J, Doyle TB, Ewald JM, Sader HS. 2024. *In vitro* development of resistance against antipseudomonal agents: comparison of novel β -lactam/ β -lactamase inhibitor combinations and other β -lactam agents. *Antimicrob Agents Chemother* 68:e0136323. <https://doi.org/10.1128/aac.01363-23>
52. Dötsch A, Schniederjans M, Khaleidi A, Hornischer K, Schulz S, Bielecka A, Eckweiler D, Pohl S, Häussler S. 2015. The *Pseudomonas aeruginosa* transcriptional landscape is shaped by environmental heterogeneity and genetic variation. *mBio* 6:e00749-15. <https://doi.org/10.1128/mBio.00749-15>
53. Rojas LJ, Yasmin M, Benjamino J, Marshall SM, DeRonde KJ, Krishnan NP, Perez F, Colin AA, Cardenas M, Martinez O, Pérez-Cardona A, Rhoads DD, Jacobs MR, LiPuma JJ, Konstan MW, Vila AJ, Smania A, Mack AR, Scott JG, Adams MD, Abbo LM, Bonomo RA. 2022. Genomic heterogeneity underlies multidrug resistance in *Pseudomonas aeruginosa*: a population-level analysis beyond susceptibility testing. *PLoS One* 17:e0265129. <https://doi.org/10.1371/journal.pone.0265129>
54. Burgaya J, Marin J, Royer G, Condamine B, Gachet B, Clermont O, Jauregui F, Burdet C, Lefort A, de Lastours V, Denamur E, Galardini M, Blanquart F, Colibafí/Septicoli & Coliville groups. 2023. The bacterial genetic determinants of *Escherichia coli* capacity to cause bloodstream infections in humans. *PLoS Genet* 19:e1010842. <https://doi.org/10.1371/journal.pgen.1010842>
55. Hu K, Meyer F, Deng Z-L, Asgari E, Kuo T-H, Münch PC, McHardy AC. 2024. Assessing computational predictions of antimicrobial resistance phenotypes from microbial genomes. *Brief Bioinform* 25:bbae206. <https://doi.org/10.1093/bib/bbae206>
56. Ben Jeddou F, Falconnet L, Luscher A, Siriwardena T, Reymond J-L, van Delden C, Köhler T. 2020. Adaptive and mutational responses to peptide dendrimer antimicrobials in *Pseudomonas aeruginosa*. *Antimicrob Agents Chemother* 64:e02040-19. <https://doi.org/10.1128/AAC.02040-19>
57. Gatzeva-Topalova PZ, May AP, Sousa MC. 2005. Structure and mechanism of ArnA: conformational change implies ordered dehydrogenase mechanism in key enzyme for polymyxin resistance. *Structure* 13:929–942. <https://doi.org/10.1016/j.str.2005.03.018>
58. Segev-Zarko LA, Kapach G, Josten M, Klug YA, Sahl HG, Shai Y. 2018. Deficient lipid A remodeling by the *arnB* gene promotes biofilm formation in antimicrobial peptide susceptible *Pseudomonas aeruginosa*. *Biochemistry* 57:2024–2034. <https://doi.org/10.1021/acs.biochem.8b00149>
59. Khaleidi A, Schniederjans M, Pohl S, Rainer R, Bodenhofer U, Xia B, Klawonn F, Bruchmann S, Preusse M, Eckweiler D, Dötsch A, Häussler S. 2016. Transcriptome profiling of antimicrobial resistance in *Pseudomonas aeruginosa*. *Antimicrob Agents Chemother* 60:4722–4733. <https://doi.org/10.1128/AAC.00075-16>
60. Arnold W, Pühler A. 1988. A family of high-copy-number plasmid vectors with single end-label sites for rapid nucleotide sequencing. *Gene* 70:171–179. [https://doi.org/10.1016/0378-1119\(88\)90115-1](https://doi.org/10.1016/0378-1119(88)90115-1)
61. Biggel M, Johler S, Roloff T, Tschudin-Sutter S, Bassetti S, Siegemund M, Egli A, Stephan R, Seth-Smith HMB. 2023. PorinPredict: *in silico* identification of OprD loss from WGS data for improved genotype-phenotype predictions of *P. aeruginosa* carbapenem resistance. *Microbiol Spectr* 11:e0358822. <https://doi.org/10.1128/spectrum.03588-22>
62. Slater CL, Winogrodzki J, Fraile-Ribot PA, Oliver A, Khajehpour M, Mark BL. 2020. Adding insult to injury: mechanistic basis for how AmpC mutations allow *Pseudomonas aeruginosa* to accelerate cephalosporin hydrolysis and evade avibactam. *Antimicrob Agents Chemother* 64:e00894-20. <https://doi.org/10.1128/AAC.00894-20>
63. Mushtaq S, Warner M, Livermore DM. 2010. *In vitro* activity of ceftazidime+NXL104 against *Pseudomonas aeruginosa* and other non-fermenters. *J Antimicrob Chemother* 65:2376–2381. <https://doi.org/10.1093/jac/dkq306>
64. Dötsch A, Becker T, Pommerenke C, Magnowska Z, Jänsch L, Häussler S. 2009. Genomewide identification of genetic determinants of antimicrobial drug resistance in *Pseudomonas aeruginosa*. *Antimicrob Agents Chemother* 53:2522–2531. <https://doi.org/10.1128/AAC.00035-09>
65. EUCAST. 2023. EUCAST: AST of bacteria. Available from: https://www.eucast.org/ast_of_bacteria. Retrieved 7 Dec 2023.
66. EUCAST. 2022. Breakpoint Tables for Interpretation of MICs and Zone Diameters, Version 12.0. Available from: https://www.eucast.org/fileadmin/src/media/PDFs/EUCAST_files/Breakpoint_tables/v_12_0_Breakpoint_Tables.pdf
67. Hughes CS, Foehr S, Garfield DA, Furlong EE, Steinmetz LM, Krijgsveld J. 2014. Ultrasensitive proteome analysis using paramagnetic bead technology. *Mol Syst Biol* 10:757. <https://doi.org/10.15252/msb.20145625>
68. Leutert M, Rodríguez-Mías RA, Fukuda NK, Villén J. 2019. R2-P2 rapid-robotic phosphoproteomics enables multidimensional cell signaling studies. *Mol Syst Biol* 15:e9021. <https://doi.org/10.15252/msb.20199021>
69. Türker C, Akal F, Joho D, Panse C, Barkow-Oesterreicher S, Rehrauer H, et al. 2010. B-Fabric: the Swiss Army knife for life sciences, p 717–720. Association for Computing Machinery, New York, NY, USA.
70. Cox J, Mann M. 2008. MaxQuant enables high peptide identification rates, individualized p.p.b.-range mass accuracies and proteome-wide protein quantification. *Nat Biotechnol* 26:1367–1372. <https://doi.org/10.1038/nbt.1511>
71. Smyth GK. 2004. Linear models and empirical bayes methods for assessing differential expression in microarray experiments. *Stat Appl Genet Mol Biol* 3:Article3. <https://doi.org/10.2202/1544-6115.1027>
72. Ritchie ME, Phipson B, Wu D, Hu Y, Law CW, Shi W, Smyth GK. 2015. Limma powers differential expression analyses for RNA-seq and microarray studies. *Nucleic Acids Res* 43:e47. <https://doi.org/10.1093/nar/gkv007>
73. Wolski W, Grossmann J, Panse C. 2021. SRMSERVICE. protViz. Available from: <https://github.com/protViz/SRMSERVICE>. Retrieved 7 Dec 2023.
74. Bolger AM, Lohse M, Usadel B. 2014. Trimmomatic: a flexible trimmer for Illumina sequence data. *Bioinformatics* 30:2114–2120. <https://doi.org/10.1093/bioinformatics/btu170>
75. Patro R, Duggal G, Love MI, Irizarry RA, Kingsford C. 2017. Salmon provides fast and bias-aware quantification of transcript expression. *Nat Methods* 14:417–419. <https://doi.org/10.1038/nmeth.4197>
76. Love MI, Huber W, Anders S. 2014. Moderated estimation of fold change and dispersion for RNA-seq data with DESeq2. *Genome Biol* 15:550. <https://doi.org/10.1186/s13059-014-0550-8>
77. Sonesson C, Love MI, Robinson MD. 2015. Differential analyses for RNA-seq: transcript-level estimates improve gene-level inferences. *F1000Res* 4:1521. <https://doi.org/10.12688/f1000research.7563.2>
78. Mölder F, Jablonski KP, Letcher B, Hall MB, Tomkins-Tinch CH, Sochat V, Forster J, Lee S, Twardziok SO, Kanitz A, Wilm A, Holtgrewe M, Rahmann S, Nahnsen S, Köster J. 2021. Sustainable data analysis with Snakemake. *F1000Res* 10:33. <https://doi.org/10.12688/f1000research.29032.2>
79. Pečar J, Lueck R, Wahlers M, European Molecular Biology Laboratory. 2020. EMBL Heidelberg HPC Cluster. Available from: <https://zenodo.org/records/12785830>. Retrieved 4 Apr 2025.
80. Jolley KA, Bray JE, Maiden MCJ. 2018. Open-access bacterial population genomics: BIGSdb software, the PubMLST.org website and their applications. *Wellcome Open Res* 3:124. <https://doi.org/10.12688/wellcomeopenres.14826.1>
81. Katz LS, Griswold T, Morrison SS, Caravas JA, Zhang S, den Bakker HC, Deng X, Carleton HA. 2019. MashTree: a rapid comparison of whole genome sequence files. *J Open Source Softw* 4:1762. <https://doi.org/10.21105/joss.01762>
82. Winsor GL, Griffiths EJ, Lo R, Dhillon BK, Shay JA, Brinkman FSL. 2016. Enhanced annotations and features for comparing thousands of *Pseudomonas* genomes in the *Pseudomonas* genome database. *Nucleic Acids Res* 44:D646–53. <https://doi.org/10.1093/nar/gkv1227>
83. Hunter JD. 2007. Matplotlib: a 2D graphics environment. *Comput Sci Eng* 9:90–95. <https://doi.org/10.1109/MCSE.2007.55>
84. Alam F, Blair JMA, Hall RA. 2023. Transcriptional profiling of *Pseudomonas aeruginosa* mature single- and dual-species biofilms in response to meropenem. *Microbiology (Reading)* 169:001271. <https://doi.org/10.1099/mic.0.001271>
85. Jacobs MA, Alwood A, Thaipisuttikul I, Spencer D, Haugen E, Ernst S, Will O, Kaul R, Raymond C, Levy R, Chun-Rong L, Guenther D, Bovee D, Olson MV, Manoil C. 2003. Comprehensive transposon mutant library of *Pseudomonas aeruginosa*. *Proc Natl Acad Sci USA* 100:14339–14344. <https://doi.org/10.1073/pnas.2036281100>
86. Chen W, Zhang Y, Zhang Y, Pi Y, Gu T, Song L, Wang Y, Ji Q. 2018. CRISPR/Cas9-based genome editing in *Pseudomonas aeruginosa* and cytidine deaminase-mediated base editing in *Pseudomonas* species. *iScience* 6:222–231. <https://doi.org/10.1016/j.isci.2018.07.024>
87. Concordet JP, Haussler M. 2018. CRISPOR: intuitive guide selection for CRISPR/Cas9 genome editing experiments and screens. *Nucleic Acids Res* 46:W242–W245. <https://doi.org/10.1093/nar/gky354>